RADIATION RESEARCH **187**, 298–318 (2017)
0033-7587/17 $15.00

DOI: 10.1667/RR4413.1

AEOL 10150 Mitigates Radiation-Induced Lung Injury in the Nonhuman Primate: Morbidity and Mortality are Administration Schedule-Dependent

Thomas J. MacVittie,[a,1] Allison Gibbs,[a] Ann M. Farese,[a] Kory Barrow,[b] Alexander Bennett,[a] Cheryl Taylor-Howell,[c] Abdul Kazi,[d] Karl Prado,[a] George Parker[e] and William Jackson III[f]

[a] *Department of Radiation Oncology, University of Maryland, School of Medicine, Baltimore, Maryland;* [b] *SNBL USA Ltd., Everett, Washington;* [c] *Clinical Research Management, Frederick, Maryland,* [d] *VA Maryland Health Care System, Baltimore, Maryland;* [e] *Charles River Laboratories, Durham, North Carolina; and* [f]*Statistician, Rockville, Maryland*

MacVittie, T. J., Gibbs, A., Farese, A. M., Barrow, K., Bennett, A., Taylor-Howell, C., Kazi, A., Prado, K., Parker, G. and Jackson III, W. AEOL 10150 Mitigates Radiation-Induced Lung Injury in the Nonhuman Primate: Morbidity and Mortality are Administration Schedule-Dependent *Radiat. Res.* 187, 298–318 (2017).

Pneumonitis and fibrosis are potentially lethal, delayed effects of acute radiation exposure. In this study, male rhesus macaques received whole-thorax lung irradiation (WTLI) with a target dose of 10.74 Gy prescribed to midplane at a dose rate of 0.80 ± 0.05 Gy/min using 6 MV linear accelerator-derived photons. The study design was comprised of four animal cohorts: one control and three treated with AEOL 10150 (n = 20 animals per cohort). AEOL 10150, a metalloporphyrin antioxidant, superoxide dismutase mimetic was administered by daily subcutaneous injection at 5 mg/kg in each of three schedules, beginning 24 ± 2 h postirradiation: from day 1 to day 28, day 1 to day 60 or a divided regimen from day 1 to day 28 plus day 60 to day 88. Control animals received 0.9% saline injections from day 1 to day 28. All animals received medical management and were followed for 180 days. Computed tomography (CT) scan and baseline hematology values were assessed prior to WTLI. Postirradiation monthly CT scans were collected, and images were analyzed for evidence of lung injury (pneumonitis, fibrosis, pleural and pericardial effusion) based on differences in radiodensity characteristics of the normal versus damaged lung. The primary end point was survival to 180 days based on all-cause mortality. The latency, incidence and severity of lung injury were assessed through clinical, radiographic and histological parameters. A clear survival relationship was observed with the AEOL 10150 treatment schedule and time after lethal WTLI. The day 1–60 administration schedule increased survival from 25 to 50%, mean survival time of decedents and the latency to nonsedated respiratory rate to >60 or >80 breaths/min and diminished quantitative radiographic lung injury as determined by CT scans. It did not affect incidence or severity of pneumonitis/fibrosis as determined by histological evaluation, pleural effusion or pericardial effusion as determined by CT scans. Analysis of the Kaplan-Meier survival curves suggested that treatment efficacy could be increased by extending the treatment schedule to 90 days or longer after WTLI. No survival improvement was noted in the AEOL 10150 cohorts treated from day 1–28 or using the divided schedule of day 1–28 plus day 60–88. These results suggest that AEOL 10150 may be an effective medical countermeasure against severe and lethal radiation-induced lung injury. © 2017 by Radiation Research Society

INTRODUCTION

Radiation-induced lung injury (RILI) is a recognized delayed effect of acute radiation exposure and is characterized by the development of pneumonitis and pulmonary fibrosis, which can lead to respiratory failure, increased morbidity and mortality. It is one of the potentially lethal sub-syndromes that follow acute radiation exposure for victims that survive the more immediate sub-syndromes of the acute radiation syndrome (ARS), including the acute gastrointestinal and hematopoietic sub-syndromes (*1–5*). Given the morbidity and mortality associated with acute radiation exposure, the development of candidate medical countermeasures (MCM) against ARS and delayed effects of multi-organ injury must be a priority (*4, 6*).

Since candidate drugs or biologics to mitigate ARS and delayed effect of acute radiation exposure cannot ethically be tested in humans, the Food and Drug Administration (FDA) has set forth guidelines regarding the design and use of surrogate animal models that provide a path to licensure for MCM under the FDA ''Animal Rule'' (*7, 8*). These criteria require: 1. An established, well-characterized animal model with a demonstrated mortality versus dose-response relationship; 2. Key signs of morbidity that are a clear representation of the human response to acute radiation; 3. The incorporated use of medical management based on prospectively defined triggers-to-treat to mimic the intended context of treatment in human clinical scenario; 4. The ability to select an effective MCM dose in humans based on

[1] Address for correspondence: University of Maryland, School of Medicine, 10 South Pine Street, Rm 6-34E, Baltimore, MD; email: tmacvittie@som.umaryland.edu.

pharmacokinetics and pharmacodynamics; 5. The ability to predict the human response to acute radiation and treatment with medical management and MCM; 6. Well-defined animal welfare-related protocols for use of sedatives, analgesia, anesthesia and euthanasia; and 7. The capability of demonstrating the desired benefit in humans (increased survival or reduction in major morbidities), when conducting an adequate and well-designed study that is blinded and randomized with adequate observation frequency. Currently, there are no FDA-approved MCM for lethal radiation-induced lung injury. A model of whole-thorax lung irradiation (WTLI) has recently been developed in the nonhuman primate (NHP) to evaluate MCM efficacy against RILI (*9, 10*). The WTLI model employed medical management that is expected to mimic the clinical context of use in a radiation accident or terrorist scenario.

Whole-thorax lung irradiation is an organ-targeted model designed to avoid the acute hematopoietic and gastrointestinal sub-syndromes, while allowing for the evaluation and characterization of potentially lethal radiation-induced damage to the lung and heart (*9, 10*). The WTLI model permits the clinical time course and biology (latency or time to onset, incidence, severity, progression and resolution) of RILI to be defined in the NHP. Additionally, the WTLI model provides an opportunity to assess the interaction of the lung and heart as a model of combined organ injury (*11–17*). In this model, the heart lies within the radiation field and receives a dose approximate to that of the lung (*15*). The concomitant irradiation of the heart is an additional risk factor for lung injury (*11–14*). The WTLI model serves as a platform for efficacy testing of candidate MCM under the criteria of the FDA Animal Rule.

The radiation-induced fibrogenic pathways associated with RILI are multifactorial, complex, dose- and time-dependent processes. Numerous MCM and cellular therapies have been assessed for mitigation of RILI and fibrosis via respective mechanisms against inflammation, oxidative stress and profibrogenic cytokines/growth factors (*18–29*). AEOL 10150 and superoxide dismutase (SOD) mimetics have focused on mitigating the pro-oxidant pathway to RILI.

The production of free radicals at the cellular level and a consequent increase in reactive oxygen and nitrogen species results in lethal lung injury after high-dose WTLI (*19, 30, 31*). Oxidative stress and the ensuing tissue injury induced by reactive oxygen species (ROS) are managed by the production of SOD. Progressive oxidative stress also plays a significant role in the initiation and incidence of chronic and delayed injuries that follow radiation exposure (*18, 19, 31*). AEOL 10150 is a small molecular weight, catalytic, metalloporphyrin antioxidant, SOD mimetic. This compound has been evaluated in murine models as a potential MCM against RILI (*19, 32–34*). AEOL 10150 was also effective in mitigating morbidity and mortality when administered daily for 28 days after a 100% lethal dose of WTLI in a pilot study using NHP (*10*).

Herein, the efficacy of AEOL 10150 to diminish the deleterious consequences of acute radiation exposure was assessed using three administration schedules after an expected 70% lethal dose in a NHP model of WTLI.

METHODS

Animals

Male rhesus macaques (*Macaca mulatta*, n = 80, Chinese origin, 5.0–10.0 kg body weight on day of irradiation) were utilized. All animals underwent quarantine for approximately 90 days and were verified to be in good health by the vendor, as seronegative for simian immunodeficiency virus, simian T-cell leukemia virus type 1, malaria and negative for herpes B virus and tuberculosis. Intradermal tuberculin testing was also performed in house during quarantine procedure. All animals were acclimated to a supine restraint device prior to WTLI. Animal housing and care have been previously described (*9*). NHP housing and care were performed in accordance with the Animal Welfare Act at the University of Maryland's Association for Assessment and Accreditation of Laboratory Animal Care-accredited animal facility.

Anesthesia

Animals were anesthetized with ketamine (Ketaset, Fort Dodge, IA) [(10 ± 5 mg/kg, intramuscularly (IM)] for procedures including initial radiation exposure, CT scans, phlebotomy, physical examinations, as well as supportive care administration, when necessary. For irradiations and CT scans, xylazine (AnaSed®; Lloyd, Inc., Shenandoah, IA) (0.5 ± 0.1 mg/kg, IM) was administered in combination with ketamine to ensure the animals would remain still for the duration of their exposure (*9, 10*).

Preirradiation Procedures and Irradiation Planning

All NHP underwent a baseline CT scan obtained in the treatment position (supine, in restraint) and a radio-opaque marker was placed just above the palpated xiphoid for reference. The external skin of the anterior chest was marked with permanent marker at this site. The pre-exposure CT scan was used to determine and plan the field of radiation to ensure inclusion of both lungs in their entirety for each individual study animal. Briefly, the CT scan was imported into the radiation planning software platform (Philips Pinnacle^3; Philips Healthcare, Andover, MA), where the lungs were contoured in 3 dimensions and an appropriate exposure plan and field size. Radiation exposure was prescribed to midplane (as opposed to a 3D lung volume) in the thorax (at the level of the xiphoid) with opposed anteroposterior (AP) and posteroanterior (PA) beams (*9, 10*).

Food was removed from each animal's cage approximately 18 h prior to exposure to reduce the likelihood of radiation-induced emesis while anesthetized. Ondansetron (Wockhardt Ltd., Parsippany, NJ; Teva Pharmaceutical, North Wales, PA; Sagent Pharmaceuticals, Schaumburg, IL) (1.5 ± 0.5 mg/kg, IV or IM) was administered 45–90 min prior to WTLI. Animals were anesthetized, placed in a Plexiglas® supine restraint device and then transported to the linear accelerator (LINAC) facility in a secure animal carrier. The eyes of the NHP were lubricated with a petrolatum ophthalmic ointment (e.g., Puralube®; Dechra Veterinary Products, Leawood, KS) prior to transport (*9*).

Irradiation and Dosimetry

Rationale for WTLI dose. Two previously published studies contributed to a defined, multiparameter dose-response relationship for mortality, the slope and y-intercept in the NHP consequent to WTLI (*9, 10*). Based on these results the WTLI dose estimate for $LD_{70/180}$ =

10.74 Gy (10.40, 11.32), with the 95% confidence intervals shown in parentheses. The dose of 10.74 Gy delivered at the prescribed midline tissue was chosen to assess the efficacy of AEOL 10150.

The primary clinically relevant end point for efficacy was an increase in survival. Our intent was to use a stringent test for efficacy with a modest number of NHP. Hence, efficacy was assessed as an increase in survival over the 70% mortality expected over the 180-day study. The proposed 70% lethality provided us approximately 40% power (one-sided) to detect a 30% reduction in lethality to 40%. Efficacy at the 30% level would provide a positive signal for efficiency relative to each AEOL 10150 treatment schedule versus the control cohort.

Whole-Thorax Lung Irradiation

NHP received a prescribed dose of 10.74 Gy WTLI, utilizing 6 MV LINAC-derived photons at a dose rate of approximately 0.80 ± 0.05 Gy/min (TrueBeam™; Varian Medical Systems Inc., Palo Alto, CA) as described previously (*9*). Briefly, the NHP were exposed in an AP/PA technique with approximately 50% dose contribution from both the AP and PA beams. To ensure accuracy of delivery, the NHP were aligned based on the xiphoid mark previously made at time of the planning CT scan, and a verification AP MV X-ray image was acquired using the LINAC's on-board imager immediately prior to exposure to verify the planned thoracic field length and width including both lungs in their entirety. Real-time *in vivo* dosimetry was confirmed with dosimeters (nanoDot™; Landauer®, Glenwood, IL) placed on each animal at time of exposure. The aforementioned real-time imaging, phantom calibration and Landauer nanoDot dosimetry ensured accurate midplane exposure.

Computed Tomography

Serial CT scans allowed the evolution of RILI to be evaluated after WTLI, both qualitatively and quantitatively. All animals underwent a baseline CT scan to plan their radiation field, and to assess radiographic evidence of preexisting lung injury or disease prior to study enrollment. Once irradiated, each NHP underwent serial CT scans for surveillance and assessment of RILI, pneumonitis/fibrosis (PF), pleural effusion (PE) or pericardial effusion (PCE) every 30 ± 5 days until the planned end of study (day 180), or until time of euthanasia ''for cause'' (IACUC criteria) prior to the end of study. Additional scans were acquired when possible, before and after post dexamethasone administration.

CT scans were acquired and analyzed as described previously using a GE Healthcare LightSpeed™ (Waukesha, WI) multi-slice CT scanner with a noncontrast enhanced thoracic protocol optimized for lung imaging (*9*). Quantification of lung injury was performed in a semiautomated fashion by using the software to assess for differences in characteristic radiodensity [as measured by Hounsfield units (HU)] and morphology for normal, pneumonitic or fibrotic lung, pleural and pericardial effusion (*9, 10, 16, 35*).

Cage-Side and Clinical Observations

Cage-side observations including nonsedated respiratory rate (NSRR) were performed twice daily by trained staff at least 6 h apart. Clinical parameters were assessed 2–3 times per week on sedated animals as previously described (*9*). The nonanesthetized respiration was obtained while the animal was in its home cage. Respiration was measured by observing the rise and fall of the chest cavity. A cycle of one inspiration and exhalation was counted as one breath. The breaths were then counted for 1 min, or a portion thereof and multiplied by the appropriate number to achieve the respiration rate per min. Respiration was also characterized by chest involvement and open-mouth breathing.

Medical Management

Medical management was provided to each NHP as per clinical signs to initiate and stop treatment (*9, 10*). Specifics on the dexamethasone paradigm are described below.

Corticosteroids for pneumonitis. Animals that developed tachypnea indicative of pneumonitis [defined as NSRR ≥80 breaths per min (bpm)], were treated with a planned corticosteroid taper. The paradigm for corticosteroid treatment and taper is described below.

First episode (first treatment course). If the NSRR increased to ≥80 bpm, dexamethasone (Butler Schein®, Dublin, OH) was administered IM using the following regimen: 1 mg/kg, twice a day (BID) on the day 1 of treatment, 0.5 mg/kg, BID for three days, 0.5 mg/kg, once a day (QD) for three days and 0.5 mg/kg every other day for three doses.

Second episode (second treatment course). If the NSRR increased to ≥80 bpm ≤7 days of the final dexamethasone dose of the first course, treatment was reinitiated as follows: 1 mg/kg, QD on the day 1, 0.5 mg/kg, QD for four days and 0.5 mg/kg every other day for ten doses (14–21 days). However, if an animal's NSRR increased again to ≥80 bpm >7 days after the final dexamethasone dose of the first course, treatment was reinitiated as follows: 1.0 mg/kg, BID on the first day, 0.5 mg/kg, BID for three days, 0.5 mg/kg, QD for three days and 0.5 mg/kg every other day for ten doses (14–21 days). Additional dexamethasone administration occurred only after a veterinarian's evaluation and treatment recommendation.

Euthanasia

Animals were euthanized with a DEA Class III euthanasia solution (Euthasol®, 0.27 ml/kg, IV; Virbac Animal Health Inc., Ft. Worth, TX). Euthanasia criteria were specified and included persistent loss of body weight, hyperthermia or hypothermia that was unresponsive to therapy, evidence of self-mutilation, evidence of unrelieved pain or stress, seizure activity, abnormal activity and respiratory distress. All staff involved in euthanasia decisions, including University veterinarians, were blinded to the treatment cohort.

Histology

Tissues procured at necropsy were processed for histological analysis as described previously using formalin-fixed and paraffin-embedded tissue (*9*). A prescribed section from each of the seven lung lobes was collected to assess the histological features and degree of pathological alterations, including collagen deposition (indicating fibrosis) by Masson's trichrome staining.

Study Design

Four NHP cohorts were used in this study, consisting of one control group and three experimental drug-treated groups (n = 20 per cohort). Each animal in all four cohorts received 10.74 Gy WTLI. The experimental drug, AEOL 10150 (5 mg/kg) was administered beginning 24 h ± 2 h postirradiation, as follows: QD for 28 days (day 1–28); QD for 60 days (day 1–60); or QD for 28 days plus no drug for 30 days plus QD for 28 days beginning on day 60 (day 1–28 plus day 60–88). Normal sterile saline (0.068 ml/kg) was administered to the control cohort QD for 28 days (day 1–28). AEOL 10150 or saline was administered by subcutaneous (SC) injection. Injection sites were rotated in a predetermined order among ten unique sites using a prescribed abdominal grid pattern.

Rationale for the Dose of and Schedule of Administration for AEOL 10150

AEOL 10150 (molecular formula C48H56Cl5MnN12) is a metalloporphyrin SOD mimetic that is currently in advanced development as a lead compound, and published findings from murine and pilot NHP studies have suggested that AEOL 10150 is

capable of improving survival after a lethal dose of WTLI (*10, 19, 32, 34*).

Rationale for Dose of AEOL 10150

The results of a published murine dose-finding study suggested that the greatest efficacy for AEOL 10150 was in the range of 10–25 mg/kg when given SC (*34*). This dose range in the mouse is the equivalent of 2.5–6.25 mg/kg in the NHP. The preclinical toxicology data (Aeolus Pharmaceuticals Inc., Mission Viejo, CA) suggested that doses greater than 6 mg/kg demonstrated cardiopulmonary effects whereas the 5 mg/kg dose was noted as the nonobservable adverse event limit. AEOL 10150 was previously tested in a pilot efficacy study in the NHP WTLI model at 5 mg/kg given SC for 4 weeks (day 1–28) after 11.5 Gy WTLI (*10*). Lethality was 100% (6/6) in the control cohort, and 71% (5/7) in the AEOL 10150-treated cohort at 180 days after WTLI. The WTLI probit-based dose-response relationship estimated that 11.5 Gy would result in >90% mortality (*9*). Therefore, the drug demonstrated efficacy in the pilot NHP study even at a high dose that proved 100% lethal in the controls (n = 6) in which the AEOL 10150-treated animals did not develop a drug dose-limiting toxicity in this study. All decedents expired secondary to radiation-induced lung damage and consequent respiratory failure. The 5 mg/kg dose of AEOL 10150 utilized in the NHP pilot study was estimated to be on the higher end of the efficacious range as predicted by the CBA murine data (*34*). There was no observable toxicity noted within the pilot study that utilized the dose of 5 mg/kg/day.

The murine data suggested that treatment at a concentration above 6.25 mg/kg (NHP equivalent dose) did not improve efficacy. Based on that information and on the above considerations it was predicted the drug would be efficacious and safe at 5 mg/kg (that drug dose used in the pilot study). The proposed dose of AEOL 10150 (5 mg/kg, QD) was chosen to provide the study herein with an estimated optimal drug effect based on the noted CBA murine data and the positive-effect pilot study in NHP.

Rationale for Administration Schedule of AEOL 10150

AEOL 10150 was initially assessed for efficacy against RILI in WTLI murine models (*32, 34, 36*), in which administration of the drug, by SC injection, was started on day 1 postirradiation and continued daily through day 28. This schedule, route and dose resulted in a consequent improvement in survival, lung function and restored expression of hypoxia-associated genes. Findings from another published study using a rat model suggested that a short one-week schedule via an osmotic mini-pump was ineffective, however, administration of AEOL 10150 for 10 weeks showed a positive response in numerous parameters in the nonlethal hemithorax exposure model (*32*). The pilot study that used AEOL 10150 at 5 mg/kg administered SC on day 1–28 was based on the above results (*10*). These studies suggested that three schedules should be assessed for efficacy: the short course of day 1–28, in an effort to replicate previous efficacy using the 28-day duration; a longer course of day 1–60, to assess the efficacy of continuous daily administration to mitigate the progressive mechanism of RILI beyond 28 days; and an intermittent course, day 1–28 plus day 60–88. The intermittent course would inform us as to whether continuous administration was required through at least the subsequent 32 days after cessation of the short 28-day course, and whether an additive, but delayed, administration of drug would mitigate the steady, continued mechanism of RILI after cessation at day 28. In effect, was a continuous, longer-term damping of the mechanism for RILI requisite for survival and diminished morbidity?

Statistical Considerations and Planned Data Analyses

The prospective longitudinal study was designed to characterize, in part, the natural course of RILI and its mitigation by administration of AEOL 10150, consequent to an expected 70% lethal dose of WTLI. The longitudinal analysis, while providing insight into radiation dose- and time-dependent morbidity and mortality, presented an unbalanced data set and potential bias due to continuous loss of NHP in control and treatment cohorts throughout the 180-day period of RILI. Statistical analysis is difficult when considering differences at selected time points due to the respective incomplete control- and treatment-cohort data sets. The number of NHP in control and treatment cohorts decreased over time after WTLI, in a cohort-dependent manner, due to the steady progression of lethal lung injury and relative efficacy of the varied treatment regimens.

The study was not statistically powered (total n = 80, n = 20/cohort) to formally compare a reasonable degree of efficacy among the four cohorts. The primary end point of the study was all-cause survival at 180 days after WTLI. It was hypothesized that overall survival of the AEOL 10150-treated cohorts at 180 days would be greater, 20–30%, than that of the control cohort. The study dataset allowed for an informed decision regarding the efficacy of the selected dose of AEOL 10150 relative to the varied administration schedules over the 180 days of the study. The 180 days all-cause mortality rates were calculated for each AEOL-treated cohort relative to schedule of administration after WTLI. Slope calculations for survival times after day 1–60 AEOL 10150 treatment from day 60 and day 90–180 were made using least squares analysis of straight line fits to data. Comparison of slopes was with an F statistic.

Analysis of the secondary end points was performed and confidence intervals (or standard errors) were calculated, where possible, for means (or medians) of select secondary end points for purposes of comparing differences over time among the four study cohorts. Other end points (some derived) and methods of analysis were used where deemed appropriate. The secondary end points included parameters that permitted the evaluation of the latency, incidence, severity, progression and resolution of RILI. These parameters were: mean and median survival time; latency to onset of tachypnea; incidence of lung injury (PF) as the percentage of animals within each cohort that, at any time, developed an increased NSRR >80 bpm and/or were found to have evidence of pneumonitis on radiographic evaluation by CT scan; radiographic lung injury (PF:TLV ratio) as the ratio of the quantified amount of lung damage (PF) based on CT scans in an animal at a given time, indexed against the total lung volume (TLV) for that animal at the time the scan was taken; and radiographic lung injury (PE:TLV ratio) as the ratio of the quantified (cc) amount of pulmonary effusion based on CT scans in an animal at a given time, indexed against the TLV for that animal at the time the scan was taken. Pericardial effusion was noted as the incidence of the quantified (cc) amount of pericardial effusion based on CT scans in an animal at a given time. Mean corticosteroid support was noted as the total amount of corticosteroid/mg provided for each animal, reported as mg of support required per day. Mean NSRR was calculated for NHP in each cohort of NHP. The mean pulse oximetry reading and mean wet lung weight for each cohort were also recorded.

Other Descriptive Statistics

Other data collected during the study that provided additional information on the pathophysiology of irradiation are presented as descriptive statistics. The difference among AEOL 10150 schedule cohorts as well as differences among survivors versus decedents within each schedule cohort is reported. Mean values are taken on the population (n size) surviving at each time point over the longitudinal, 180-day study duration. These data include: the influence of corticosteroid supportive care on the timing and amount of corticosteroid support; and influence on both clinical [NSRR, oxygen saturation (SpO_2)] and radiographic (PF on CT imaging) parameters.

TABLE 1
Percentage Lethality, Decedents/Total NHP and Mean and Median Survival Time of Decedents, Overall Survival Time and Survival Probability after WTLI in NHP Administered AEOL 10150

Treatment course	Control Day 1–28	AEOL 10150 Day 1–28	AEOL 10150 Day 1–60	AEOL 10150 Day 1–28 plus day 60–88
Percentage lethality at 180 days	75%	70%	50%	80%
Decedents/total	15/20	14/20	10/20	16/20
Mean survival time of decedents (days)	106.5 ± 11.7	100.3 ± 11.0	116.9 ± 13.6	106.3 ± 11.3
Median survival time of decedents (days)	101	98	123	100
Mean survival time of all animals (days)	125.6 ± 11.5	124.9 ± 11.5	150.0 ± 10.1	121.6 ± 11.4
Median survival time of all animals (days)	131	112	174	119
Analysis of time to event	-	$P = 0.37$	$P = 0.06$	-
Survival probability		$P = 0.396$	$P = 0.04$	$P = 0.392$

Notes. Rhesus macaques received 10.74 Gy WTLI with 6 MV LINAC-derived photons at a dose rate of 0.80 Gy/min. Rhesus macaques were administered control saline and AEOL 10150 in three different treatment schedules: AEOL 10150 day 1–28, day 1–60, and day 1–28 plus day 60–88. Animals were observed in a longitudinal analysis over the 180-day study duration postirradiation. The data suggest that AEOL 10150 had a schedule-dependent effect on the survival probability, survival time of decedents and overall survival time per cohort. All cohorts represent an unbalanced data set relative to the baseline (n = 20/cohort) due to time- and drug-dependent morbidity and mortality throughout the study duration. The mean survival times are presented ± standard error.

RESULTS

Survival

The primary end point of the study was survival at 180 days after 10.74 Gy WTLI, an estimated $LD_{70/180}$. The cumulative mortality associated with each of the cohorts herein at day 180 was: controls day 1–28, 75% (15/20); AEOL 10150 day 1–28, 70% (14/20); AEOL 10150 day 1–60, 50% (10/20); and AEOL 10150 day 1–28 plus day 60–88, 80% (16/20) (Table 1, Fig. 1). Findings from the time-to-event analysis for survival over the 180 days of the study revealed the following, relative to the 25% survival of the control cohort: the AEOL 10150 day 1–60 cohort had increased survival to 50% ($P = 0.06$, one-sided, mid P

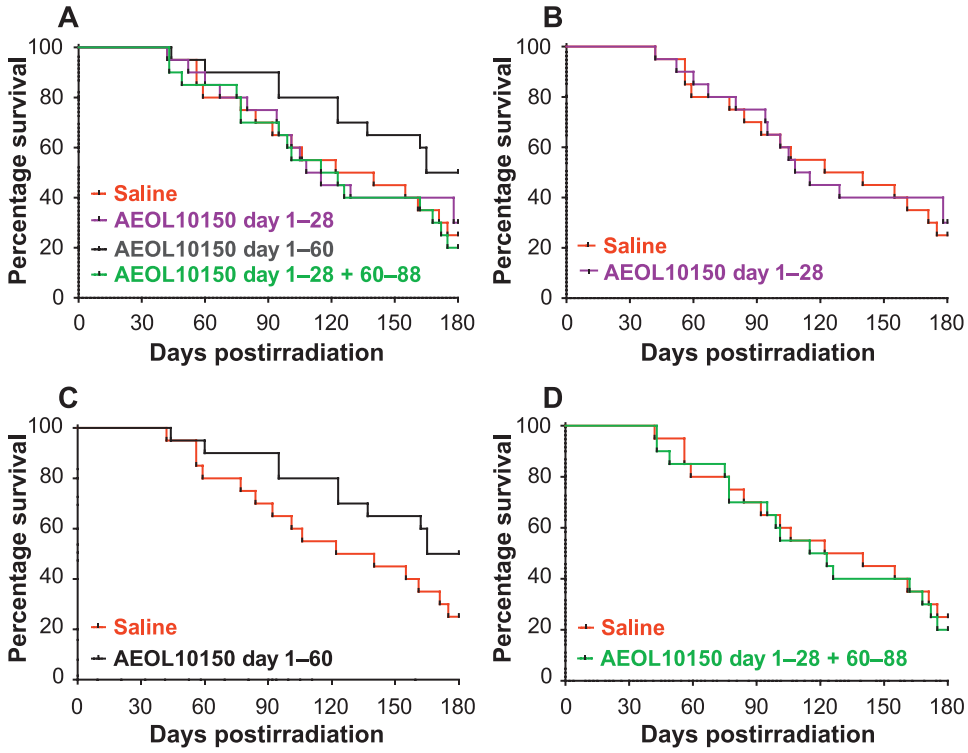

FIG. 1. Kaplan-Meier survival curves demonstrating schedule-dependent outcome over time for all 10.74 Gy WTLI NHP cohorts. Survival over 180 days is plotted for the control (saline) and each AEOL 10150-treated cohort. Panel A: All cohorts; panel B: AEOL 10150 day 1–28 cohort. Panel C: AEOL 10150 day 1–60. Panel D: AEOL 10150 day 1–28 plus day 60–88 cohort. Comparison of the survival curves, using the one-sided, exact log-rank test, showed significant difference ($P = 0.042$) in the survival probability of the AEOL 10150 day 1–60 cohort relative to the control.

value, Fisher's exact test); the AEOL 10150 day 1–28 cohort had increased survival to 30% ($P = 0.37$); and the cohort that received AEOL 10150 on day 1–28 plus day 60–88 showed 20% survival (Table 1).

Analysis of the Kaplan-Meier survival curves confirmed the survival effect observed over the entire 180-day serial time course. The survival probability noted for the AEOL 10150 day 1–60 cohort was significantly different from the control cohort ($P = 0.042$, one-sided, exact log rank test), whereas the survival effect observed with the AEOL 10150 day 1–28 cohort was not significant relative to the control cohort ($P = 0.392$), as also noted for the AEOL 10150 day 1–28 plus day 60–88 cohort ($P = 0.396$) (Table 1, Fig. 1). The earliest mortality (time-to-event) was noted within the second month postirradiation for all cohorts. The probability of surviving the initial 60-day interval postirradiation ranged from 0.80 (16/20) to 0.90 (18/20). The increased mortality over the subsequent 30-day interval shifted the probability of survival over the cumulative day 1–90 interval in favor of the day 1–60 AEOL 10150 administration schedule, which remained at 0.90 relative to 0.70 (for control), 0.75 (for day 1–28 AEOL 10150 cohort) and 0.70 (day 1–28 plus day 60–88 AEOL 10150 cohort). The slopes for the day 1–60 AEOL 10150 cohort versus the control cohort were significantly different from the time interval at day 60–180, $P = 0.0012$. The survival probability within the control, AEOL 10150 day 1–28 and day 1–28 plus day 60–88 cohorts continued at equivalent rates. The AEOL 10150 day 1–60 schedule mitigated the ''early'' mortality rate and increased cumulative survival to 50% at day 180, suggesting that extended administration of AEOL 10150 may be required to further diminish the mortality rate and increase survival across the 180-day study duration. It is of interest that the slope for survival probability for the day 1–60 AEOL 10150 cohort reverted to that of the control cohort and other AEOL 10150-treated cohorts from the 90-day time interval through the 180-day study duration ($P = 0.39$). The mechanism for RILI remained persistent through the 180-day time point. The divided AEOL 10150 administration schedule further suggested that the delayed administration did not compensate for apparent loss of AEOL 10150 mitigation and progression of RILI during the second month after WTLI. The lethal course of RILI had been established over the initial 60 days postirradiation.

Secondary End Points

Mean and median survival time of decedents; overall mean and median survival time. The mean survival time of decedents was increased, though not significantly, in the AEOL 10150 day 1–60 cohort at 116.9 ± 13.6 days relative to the control cohort (106.5 ± 11.7 days) or the other AEOL 10150 cohorts, day 1–28 (100.3 ± 11.0 days) and day 1–28 plus day 60–88 (106.3 ± 11.3 days). The overall mean survival time for each cohort was 125.6 ± 11.5 days for the control, and for each AEOL 10150-treated cohort (in parentheses), 124.9 ± 11.5 days (day 1–28), 150.0 ± 10.1 days (day 1–60) and 121.6 ± 11.4 days (day 1–28 plus day 60–88) (Table 1).

Median survival times for decedents (with cohort in parentheses) were: 101.0 days (control), 98.0 days (AEOL 10150 day 1–28), 123.0 days (AEOL 10150 day 1–60) and 100.0 days (AEOL 10150 day 1–28 plus day 60–88) (Table 1). The median values for overall survival time (all animals) were (with cohort in parentheses): 131 days (control), and for the AEOL 10150-treated cohorts, 112 (day 1–28), 174 (day 1–60) and 119 days (day 1–28 plus day 60–88). The AEOL 10150 day 1–60 cohort had the highest mean and median survival time of decedents and overall survival time relative to the control and other AEOL 10150-treated cohorts (Table 1). These values suggest that the progression of lethal RILI was delayed by the 60-day administration of AEOL 10150 relative to no AEOL 10150 treatment or other AEOL 10150 treatment schedules.

Latency or time to onset and incidence of clinical evidence of pneumonitis: NSRR ≥60 bpm and ≥80 bpm, over study duration. The NSRR tracked similarly for all NHP, survivors and nonsurvivors, in all cohorts through approximately 45 days after WTLI. The NSRR began to rise within the first several weeks after WTLI irrespective of treatment with AEOL 10150 (Fig. 2A). Separation of the cohorts into survivors and nonsurvivors revealed a modest separation of NSRR in the survivor cohorts relative to the nonsurvivors (Fig. 2B and C). The NSRR for the treated cohorts remained less than control over the approximate time frame of 40–130 days postirradiation, after which all surviving cohorts maintained equivalent NSRR >60 bpm (Fig. 2A–C). The NSRR for the nonsurvivor cohorts were equivalent relative to control over the time course of RILI.

Overall incidence of clinical/radiographic indications of lung injury. The incidence for clinical evidence of pneumonitis for the control and each treatment cohort was calculated and is presented as percentage of total NHP with NSRR ≥80 in each cohort. Overall incidence over the time course in the control cohort was 85%, relative to 65%, 90% and 80% in the AEOL 10150-treated cohorts (day 1–28, day 1–60 and day 1–28 plus day 60–88, respectively; Table 2). All NHP with a NSRR ≥80 had correlative CT-based radiographic evidence of injury. We note that the mean values over the time course are edited by the respective loss of nonsurviving NHP.

NSRR ≥60 bpm. A NSRR ≥60 bpm was early clinical evidence of the progression of RILI. The mean day 1 to an NSRR ≥60 for all NHP in each cohort was 48, 49, 68 and 52 days for the control and respective AEOL 10150 cohorts day 1–28, day 1–60 and day 1–28 plus day 60–88 relative to mean baseline respiration rate values of 37, 35, 36 and 37 bpm. The median values for the day 1 to NSRR ≥60 were 44 days for the control cohort and 41, 62 and 46 days for the respective AEOL 10150 cohorts day 1–28, day 1–60 and day 1–28 plus day 60–88 (Table 3). These data suggest that administration of AEOL 10150 for 60 days delayed the

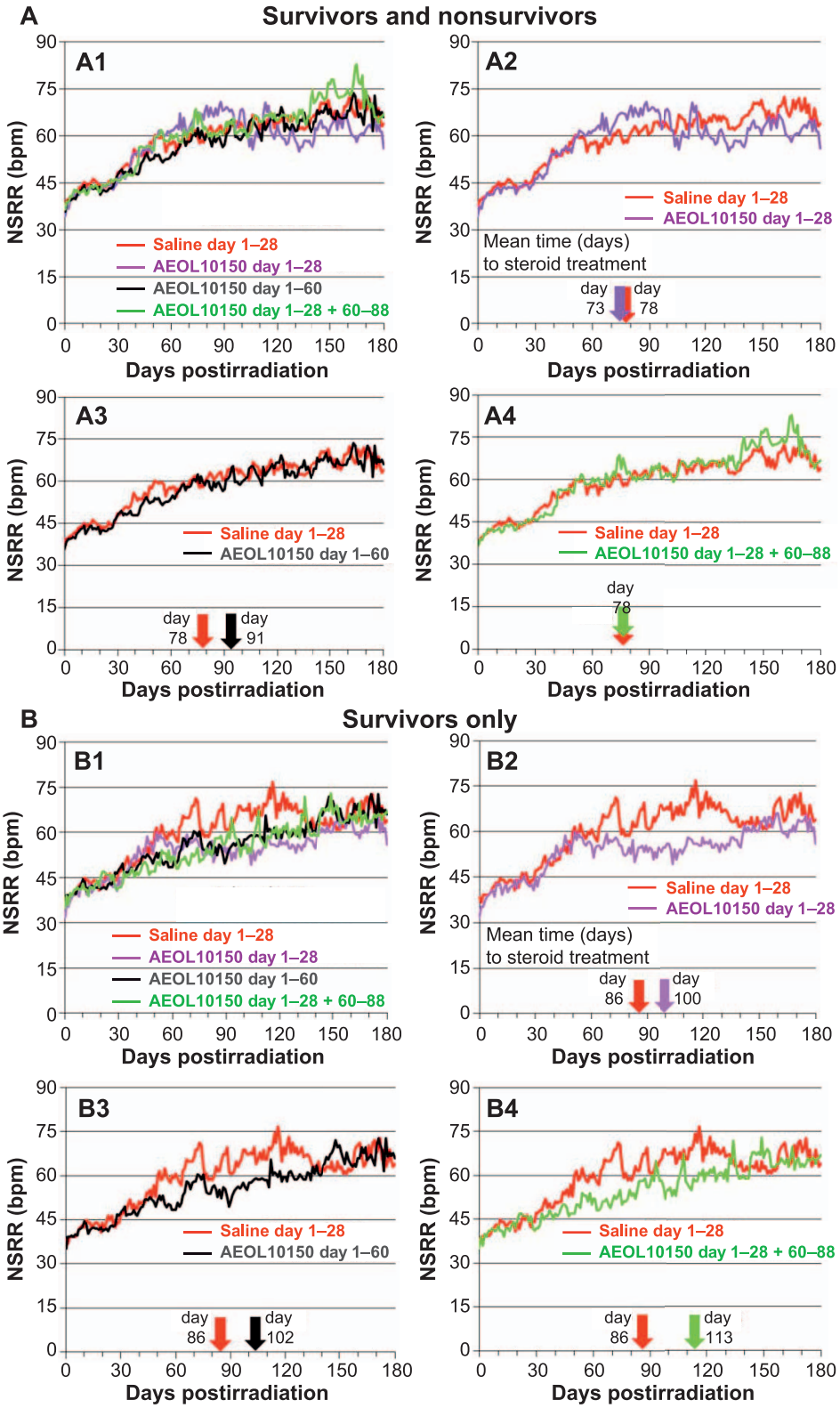

FIG. 2. Panel A: Comparison of mean nonsedated respiratory rates (NSRR) over time for all NHP survivors and nonsurvivors in the control (saline) cohort and each AEOL 10150-treated cohort. Note: NHP numbers decreased with time due to continued morbidity and mortality over the entire study duration (see Fig. 6A). Panel A1: All NHP control and AEOL 10150-treated cohorts. Panels A2–A4: Control vs. each AEOL 10150-treated cohort. The color-coded arrows along the x-axis denote the mean day 1 of steroid treatment for respective cohorts. Dexamethasone was administered for animals that developed clinical signs for pneumonitis defined as tachypnea, NSRR $\geq$80. Panel B: Comparison of mean NSRR over time for the control (saline) cohort and each AEOL 10150-treated cohort, for survivors only. Panel B1: All surviving NHP control vs. AEOL 10150-treated cohorts. Panels B2–B4: Control vs. each AEOL 10150-treated cohort. The color-coded arrows along the x-axis denote the mean day 1 of steroid treatment for respective cohorts. Dexamethasone was administered for animals that developed clinical signs for pneumonitis defined as tachypnea, NSRR $\geq$80.

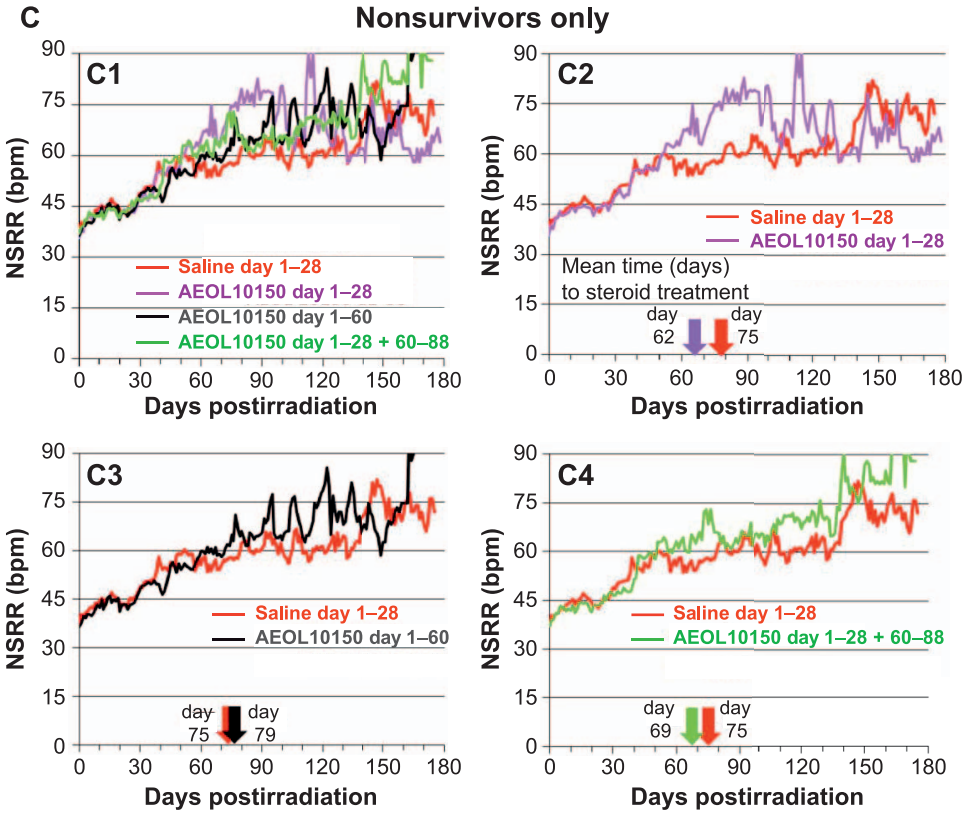

FIG. 2. (Continued) Panel C: Comparison of mean NSRR over time for the control (saline) and each AEOL 10150-treated cohort, for nonsurvivors only. Panel C1: All nonsurviving NHP control vs. AEOL 10150-treated cohorts. Panels C2–C4: Control vs. each AEOL 10150-treated cohort. The color-coded arrows along the x-axis denote the mean day 1 of steroid treatment for respective cohorts. Dexamethasone was administered for animals that developed clinical signs for pneumonitis defined as tachypnea, NSRR ≥80.

early clinical manifestation of RILI relative to control and other treatment cohorts.

NSRR ≥80 bpm. Clinically significant pneumonitis was defined as having a NSRR ≥80 bpm, at which point NHP received dexamethasone treatment as described in Methods. The mean day 1 to an NSRR ≥80 for all NHP in each cohort was 78 days for controls and 73, 91 and 78 days for the respective AEOL 10150 cohorts day 1–28, day 1–60 and day 1–28 plus day 60–88 relative to mean baseline NSRR of 37, 35, 36, and 37 bpm. The median days the NSRR was ≥80 were 73, 62, 79 and 77 days for saline- or AEOL 10150-treated cohorts day 1–28, day 1–60, and day 1–28 plus day 60–88, respectively (Table 3). The AEOL 10150 day 1–60 cohort had the longest mean and median latency or time to onset from baseline to NSRR ≥60 or ≥80 bpm relative to the control and other AEOL 10150 cohorts. All control and AEOL 10150-treated cohorts, survivors and nonsurvivors, showed clinical evidence of pneumonitis over the study duration.

NSRR ≥60 bpm, ≥80 bpm; earliest day to onset after WTLI. The longitudinal analysis revealed that while all NHP showed increased NSRR, the incidence of NHP reaching either threshold for NSRR was the lowest in the AEOL 10150 day 1–60 cohort. The AEOL 10150 administration in the day 1–60 cohort was more effective in reducing the number (2/20, 10%) of NHP reaching an NSRR ≥60 bpm relative to control and other AEOL 10150-treated cohorts. The time to reach an NSRR ≥80 bpm also occurred later in

TABLE 2
Percentage and Incidence of Rhesus Macaques Having a NSRR ≥80 after WTLI

	Survivors		Decedents		Cohort	
Treatment course	Percentage	n/N	Percentage	n/N	Percentage	n/N
Saline (day 1–28)	100	5/5	80	12/15	85	17/20
AEOL 10150 (day 1–28)	67	4/6	64	9/14	65	13/20
AEOL 10150 (day 1–60)	90	9/10	90	9/10	90	18/20
AEOL 10150 (day 1–28 plus day 60–80)	75	3/4	81	13/16	80	16/20

Notes. The NSRR was obtained twice daily after WTLI through the end of the study, day 180 or when euthanasia occurred. Percentage and incidence (n/N) in each treatment cohort are presented as the survivors, survived to the end of the study, day 180; the decedents, died or euthanized for cause prior to day 180 and the entire treatment cohort regardless of survival status.

TABLE 3
Day 1 and Incidence to a NSRR ≥60, ≥80

Treatment course	Mean Baseline NSRR	Day 1 of NSRR ≥60 bpm						Day 1 of NSRR ≥80 bpm					
		Mean ± SEM			Median			Mean ± SEM			Median		
	All[a]	Survivors	Decedents	All[a]	Survivors	Decedents	All[a]	Survivors	Decedents	All[a]	Survivors	Decedents	All[a]
Saline (day 1–28)	37	46 ± 5	48 ± 6	48 ± 5	44	43	44	86 ± 15	75 ± 9	78 ± 8	72	76	73
AEOL 10150 (day 1–28)	35	55 ± 11	46 ± 4	49 ± 4	40	50	41	100 ± 24	62 ± 9	73 ± 10	94	54	62
AEOL 10150 (day 1–60)	36	79 ± 15	57 ± 7	68 ± 9	64	47	62	102 ± 14	79 ± 7	91 ± 8	80	77	79
AEOL 10150 (day 1–28 plus day 60–80)	37	61 ± 9	50 ± 6	52 ± 5	57	45	46	113 ± 12	69 ± 7	78 ± 8	117	55	77

Notes. The NSRR was obtained twice daily after WTLI through the end of the study, day 180 or when euthanasia occurred. The latency (mean ± standard error, and median values) to clinical evidence of development of pneumonitis (NSRR ≥60, ≥80) after WTLI in the NHP model is described. Each treatment cohort is presented as survivors, survived to the end of the study, day 180; decedents, died or euthanized for cause prior to day 180 and all NHP in the entire treatment cohort regardless of survival status.

[a] All NHP in cohort.

the AEOL 10150 day 1–60 cohort (91 days) relative to control (78 days) and other AEOL 10150 cohorts, day 1–28, and day 1–28 plus day 60–88 (day 73 and 78, respectively) (Table 3). The AEOL 10150 day 1–60 cohort recorded the longest time to onset of NSRR ≥60 bpm, or ≥80 bpm relative to the control and other AEOL 10150 cohorts. This lends support to the requirement for 60 days of continuous treatment to mitigate the increase in NSRR and lethal progression of radiation dose-dependent RILI.

Mean dexamethasone support. Treatment with a planned dexamethasone taper was initiated as a part of medical management for NHP who developed clinical evidence of pneumonitis (NSRR ≥80 bpm). Animals with greater radiation-induced injury triggered dexamethasone support more frequently, and therefore the total amount of dexamethasone an animal received during the study was considered a reliable surrogate for the severity of radiation-induced lung injury. Survival time certainly had a positive influence on the opportunity to prompt dexamethasone treatment. Therefore, the required dexamethasone support was calculated as mg/kg received per survival time (Table 4). In this context, all treatment cohorts received an equivalent amount of dexamethasone support.

Nonsedated respiratory rate and dexamethasone treatment. The mean values of daily NSRR for all cohorts and for all NHP/cohort both survivors and nonsurvivors/cohort,

TABLE 4
Dexamethasone Support in Rhesus Macaques after WTLI

Treatment course	Dexamethasone treated			All NHP	
	No. treated (n/N)	Average mg/kg/day per days alive	Average no. of courses	Average mg/kg/day per days alive	Average no. of courses
A[1]					
Saline (day 1–28)	18/20	0.029	1.9	0.026	1.8
AEOL 10150 (day 1–28)	13/20	0.040	2.7	0.026	1.8
AEOL 10150 (day 1–60)	18/20	0.038	2.8	0.034	2.5
AEOL 10150 (day 1–28 plus day 60–80)	17/20	0.039	2.5	0.033	2.2
B[2]					
Saline (day 1–28), survivors	5/5	0.035	2.6	0.035	2.6
Saline (day 1–28), nonsurvivors	13/15	0.027	1.7	0.023	1.5
AEOL 10150 (day 1–28), survivors	4/6	0.021	2.0	0.014	1.3
AEOL 10150 (day 1–28), nonsurvivors	9/14	0.049	3.0	0.031	1.9
AEOL 10150 (day 1–60), survivors	9/10	0.040	3.1	0.036	2.8
AEOL 10150 (day 1–60), nonsurvivors	9/10	0.036	2.4	0.033	2.2
AEOL 10150 (day 1–28 plus day 60–88), survivors	3/4	0.035	3.0	0.026	2.3
AEOL 10150 (day 1–28 plus day 60–88), nonsurvivors	14/16	0.040	2.4	0.035	2.1

Notes. Dexamethasone was calculated as the mean dosage (mg/kg/day during study days alive) administered for each treatment cohort, control (saline) and AEOL 10150 for day 1–28, day 1–60, and day 1–28 plus day 60–88. Rhesus macaques were administered dexamethasone when the NSRR increased to ≥80 bpm in a prescribed treatment paradigm after 10.74 Gy WTLI.

[1] A = Calculations were performed two ways: Considering only the NHP that triggered dexamethasone in each cohort; and considering all NHP in each cohort. The amount of steroid support required was similar across all cohorts regardless of treatment in the study.

[2] B = Calculations of dexamethasone support are shown per survivors and nonsurvivors for each cohort, control and schedule-dependent AEOL 10150 treatment.

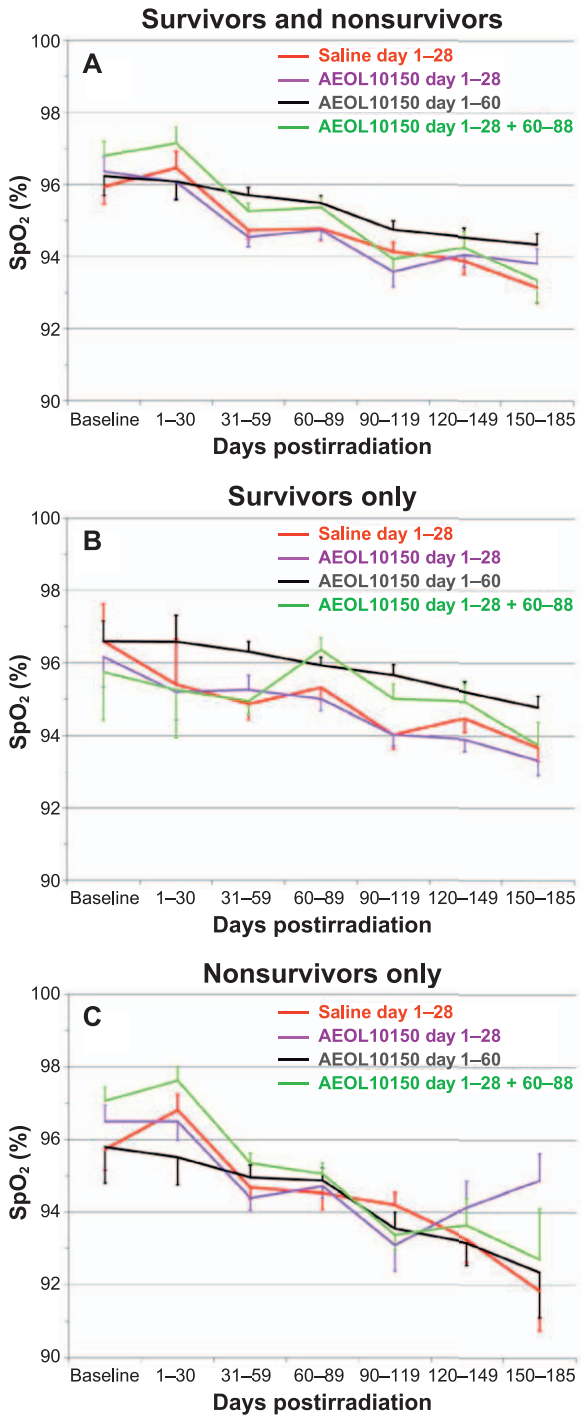

FIG. 3. Mean pulse oximetry (SpO_2) levels over the study duration of 180 days after WTLI for the control (saline) and all AEOL 10150-treated cohorts: day 1–28, day 1–60 and day 1–28 plus day 60–88. Note: NHP numbers decreased with time due to continued morbidity and mortality over the entire study duration (See Fig. 6A.) Panel A: Comparison of SpO_2 over time for all NHP (survivors and nonsurvivors) control and AEOL 10150-treated cohorts. Panel B: Comparison of SpO_2 over time for NHP (survivors only) control and AEOL 10150-treated cohorts. Panel C: Comparison of SpO_2 over time for NHP (nonsurvivors only) control and AEOL 10150-treated cohorts.

trended higher over time after 10.74 Gy WTLI, an estimated $LD_{70/180}$ (Fig. 2A–C). However, the mean NSRR was influenced by dexamethasone treatment, as well as the continuing lethality of the most severely injured animals and therefore diminished the ''n/cohort'', throughout the 180-day study duration.

Dexamethasone administration. Dexamethasone was generally effective in temporarily palliating the symptoms of radiation-induced pneumonitis as reflected in secondary end points such as NSRR and radiographic CT evidence of lung injury. Graphically, this mitigation is evident when one overlays the mean latency to onset of clinical pneumonitis (e.g., initial dexamethasone treatment) with the mean NSRR plot (Fig. 2A–C). This is also demonstrated in the context of the steroid effect on the severity of radiographic lung injury. The average timing of the first dexamethasone administration (NSRR $\geq$80 bpm) for the control cohort was 78 days, and for the AEOL 10150-treated cohorts (in parentheses), 73 days (day 1–28), 91 days (day 1–60) and 78 days (day 1–28 plus day 60–88) (Table 2).

The timing of the initial dexamethasone administration (mean values) for all animals correlated well with the increased efficacy in survival (50%) and longer latency for day 1 to an NSRR $\geq$80 bpm (91 days) noted for the AEOL 10150 day 1–60 cohort relative to the control (25% survival, 78 days latency) and other AEOL 10150 cohorts (day 1–28: 30% survival, 73 days latency; day 1–28 plus day 60–88: 20% survival, 78 days latency) (Tables 1 and 3).The overall administration of dexamethasone was equivalent relative to all treatment cohorts. However, latency or the mean time to administration of dexamethasone was the greatest for the AEOL 10150 day 1–60 cohort relative to the control and other AEOL 10150-treated cohorts. The median value was also slightly higher than for the control and other AEOL 10150-treated cohorts.

Pulse oximetry. The change in SpO_2 was an indicator of compensated respiratory function. The mean SpO_2 was calculated for all NHP within each cohort (Fig. 3A–C). The trend toward higher SpO_2 values, indicative of less hypoxia, was noted with the AEOL 10150 day 1–60 cohort over the 180-day study duration relative to that noted for the control cohort when viewed in terms of all NHP and the survivor cohort (Fig. 3B). The SpO_2 values were equivalent within the nonsurvivor cohorts, indicating all nonsurvivors in control and AEOL 10150-treated cohorts had difficulty compensating for hypoxia induced by the expected 70% lethal dose in WTLI (Fig. 3C). This effect was also reported in a previous pilot study (*10*). Lethality in the WTLI model was consequent to pulmonary injury and respiratory failure. Hypoxia, as evidenced by low SpO_2, was the most common single (64%) euthanasia criteria met for decedent NHP in this and other contemporary comparative studies in NHP (*9, 10*).

Radiographic analysis: incidence, time course and severity of lung injury and pericardial effusion. Non-contrast-enhanced CT scans were obtained approximately

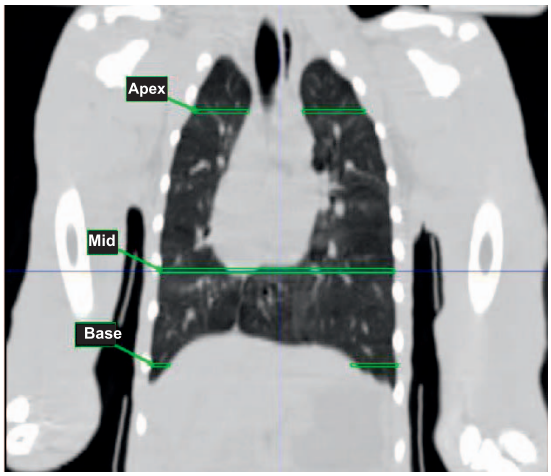

FIG. 4. Coronal view of baseline in a NHP, indicating approximate areas where serial CT images, labeled apex, mid and base, were obtained.

every 30 days starting at day 30 after WTLI. Serial CT scans, images at the apex, mid and base were then analyzed for the presence and severity of pneumonitis/fibrosis (PF) and pleural- (PE) or pericardial effusions (PCE) to determine their latency, incidence, severity and progression of lung injury through the study duration (Figs. 4, 5A and B). The incidence of PF, PE and PCE was calculated for all cohorts (Table 5).

The normal lung volume (LV) subtracted from the total (TLV) yielded the injured lung volume and was representative of PF. The PE and PCE were contoured as separate volumes and distinguished based on characteristic differences in radiodensity. Since pulmonary effusions generally layer with gravity and have a radiodensity that approximates that of water (HU = 0), they could be evaluated using the ''HU fat-water-tissue'' anatomical view on the MIM® Software program (Cleveland, OH) (Fig. 4) (*9*). It was important to index the injury against the TLV for each scan, because the TLV was usually variable from scan to scan based on the dominant phase of respiration at the time of scan acquisition, growth that occurred during the 180-day life phase of the study and size differences among NHP (*9*). The PCE was identified around the heart by using the ''fat-water-tissue'' viewing, as with the pulmonary effusions (*9, 16*). Consideration of these factors allowed for the most realistic longitudinal, quantitative assessment of RILI based on CT scan analysis.

Evolution of radiographic changes: PF:TLV, PE:TLV. Radiographic evidence of RILI as PF and PE evolved with time over the 180-day study duration after lethal WTLI in all NHP. Serial images were obtained at three different locations in the lung, apex, mid-lung and base from a surviving NHP euthanized at the end of the 180-day study duration and a nonsurvivor euthanized at 101 days after WTLI (Fig. 5A and B). These figures provided evidence of the marked regional heterogeneity in tissue damage during the progression of RILI in lungs of representative NHP. Results were reported quantitatively as ratios (PF:TLV and PE:TLV) and represented the percentage of lung that appeared injured (PF) or acquired PE at the time the CT scans were taken over the respective time course after WTLI.

Dexamethasone treatment is known to influence lung injury and its radiographic appearance (*9, 10, 37–40*). This, as well as the fact that all NHP survived through day 30 postirradiation, render the day 30 CT scan assessment the only image analysis time point where all experimental cohorts are free of confounding influence of dexamethasone support and ongoing mortality that resulted in unbalanced, time-dependent loss of NHP per cohort through 180 days postirradiation. The radiographic images show the presence of PF, PE and the use of dexamethasone and furosemide administered according to protocol (Fig. 5A and B). Dexamethasone was administered based on NSRR and furosemide was administered by veterinary prescription, based only on response to clinical observations.

PF:TLV: overall incidence of radiographic injury. The longitudinal data revealed the resolute presence of RILI in all control and AEOL 10150-treated NHP regardless of administration schedule (Table 5; Fig. 6A–C). Radiographic evidence of PF was evident at the initial CT scans at 30 days postirradiation and ranged from 20% to 55% across all control and AEOL 10150-treated cohorts. The incidence of PF increased to 100% over the study duration for all animals in three cohorts: control; AEOL 10150 day 1–60; and AEOL 10150 day 1–28 plus day 60–88. There was 86.7% incidence of PF observed in the AEOL 10150 day 1–28 cohort (Table 5).

Percentage PF:TLV. The mean values for quantitative lung injury reported as percentage PF:TLV over the 180-day study duration revealed an expected lower trend in values (although not significant) with time postirradiation for the AEOL 10150 day 1–60 cohort relative to the control and AEOL 10150 day 1–28 cohorts when viewed in the context of all NHP, combined survivors and nonsurvivors (Fig. 6A). The PF:TLV database suggested that the extent or amount of pneumonitis and/or fibrosis as judged by radiographic evidence was not significantly different among the cohorts when viewed over time postirradiation. Note that the longitudinal database included a diminished number of NHP per cohort, 50–65%, over the 180 days postirradiation. The PF:TLV mean values for lung injury for all NHP (survivors and nonsurvivors) increased to reach a plateau from 90 to 180 days postirradiation. Examination of the time course of injury within the surviving NHP revealed an equivalent, although lesser degree of, persistent injury among all cohorts as well as a delayed rise in injury at approximately 90 days across all the cohorts relative to that observed for the nonsurvivor cohorts (Fig. 6B and C). The longitudinal analysis of PF:TLV while edited over the time course due to continued loss of NHP in all cohorts to lethal RILI indicated that the extent of PF is equivalent within all cohorts, survivors or nonsurvivors, over the 180-day time

course. These data correlate well with the rise in NSRR and decrease in SpO_2 (Figs. 2 and 3). The longitudinal analysis demonstrated the intractable increase in lung injury consequent to a 70% lethal dose of radiation to lung and heart.

PE:TLV: Overall incidence of radiographic injury; percentage PE:TLV. The incidence of PE increased within 30 days after WTLI and ranged from 50% to 75% across all cohorts, control and AEOL 10150-treated (Table 5; Fig. 7A–C). The data suggested an equivalent incidence and mean values for percentage PE:TLV although there was variable severity (volume) of PE at any time point within each of the cohorts, as well as within survivors and nonsurvivors (Fig. 7A–C). The severity and incidence are notable between survivors and nonsurvivors. The PE resolved in the survivors within approximately 90 days postirradiation and 120 days in nonsurvivors without correlation to AEOL 10150 administration schedule. The mean PE volume (ml), measured during the peak 30–90 days, was consistent across all cohorts, ranging from 7–31 ml. PE detected thereafter from 120–180 days was modest and ranged from $\leq$0.06–0.63 ml.

Pericardial effusion: incidence, time to onset, volume. The incidence of PCE, which occurred predominantly within 60 days after WTLI in all animals (Table 5), ranged from 12.5% to 37.5% at 60 days and remained present through 90 days postirradiation in all except the AEOL 10150 day 1–28 cohort. The PCE declined thereafter through the end of the 180-day study duration. These values corresponded to the radiographic evidence of PCE where the mean day to onset was 68 days for the control cohort and 75, 71 and 60 days for the AEOL 10150 day 1–28, day 1–60 and day 1–28 plus day 60–88 cohorts, respectively. The PCE volume was variable across all cohorts.

Lung weight. To account for differences in the sizes and ages of the NHP, a ratio of the wet lung weight (LW) and the body weight (BW) was calculated and then averaged for each treatment cohort, and then further divided based on survivors versus nonsurvivors. The mean LW:BW ratio (0.815%) of six naïve, nonirradiated animals was obtained and defined as 1.00. To demonstrate the lung weight gain due to accumulated parenchymal damage and edema after WTLI, the mean of LW:BW ratios between the irradiated and normal animals were compared (Table 6). The LW:BW ratio, observed at necropsy, was the lowest in the AEOL 10150 day 1–60 cohort compared to the ratios of all animals in each cohort, as well as the ratios of survivors and decedents in each cohort (Table 6). The values for all animals in each cohort ranged from 1.322 to 1.566 for three cohorts (control, AEOL 10150 day 1–28 and AEOL 10150 day 1–28 plus day 60–88), whereas the lowest ratio, 1.322 was noted in the AEOL 10150 day 1–60 cohort. It was observed that the surviving NHP had lower mean LW:BW ratios compared with decedents, with the exception of the AEOL 10150 day 1–60 cohort, which had the lowest LW:BW ratio in both survivors and decedents. The AEOL 10150 day 1–60 cohort survivors had a LW:BW ratio of 1.306, whereas the decedents had a ratio of 1.341. Notably, the decedents in the control and remaining AEOL 10150 cohorts had higher LW:BW ratios that ranged between 1.568 to 1.613 (Table 6).

Histological evaluation. Although lung tissue was reviewed from all NHP, a single consistent problem with assessing tissue pathology in the lung is that the radiation-induced damage is markedly heterogeneous and focal in location, time to onset, severity and extent in each animal. Therefore, a strict prospective protocol for tissue procurement was imperative. A minimum of seven samples were procured from the lung of each NHP ($n = 80$). Specimens from each of the seven major lung lobes were collected from similar locations within the individual lung lobes, and with similar orientation relative to lung surfaces and pneumovascular tracts. The radiation-induced histological alterations that evolved over 180 days would be influenced by the MCM administration schedule and individualized medical management based on clinical signs, e.g., dexamethasone. Additionally, NHP from all treatment cohorts were euthanized at different points along the 180-day period.

Overview of histopathology at all euthanasia intervals. The H&E-stained lung sections of NHP from all treatment cohorts had a constellation of changes that included accumulation of proteinic fluid within alveolar lumina, infiltration of mononuclear cells (MNC) and neutrophils, accumulations of alveolar macrophages and bronchioloalveolar hyperplasia. The constellation of changes tended to be most pronounced in the upper and middle lobes of the lungs, although lower and intermediate lobes were not completely spared. The various pathological components were focally or multifocally distributed within each lung lobe, as opposed to diffuse throughout the sections, and had no discernible pattern of distribution relative to lung surfaces, airways or vasculature.

The Masson's trichrome-stained sections had increased focally or multifocally distributed collagen that was recorded as interstitial fibrosis. It was commonly co-located with infiltrations of neutrophils, mononuclear inflammatory cells or alveolar macrophages, and was more pronounced in the upper and middle lung lobes.

Salient Histopathological Features at Euthanasia Intervals after WTLI

Day 42–60. Histological changes consisted primarily of accumulations of alveolar proteinic material with MNC, neutrophil and macrophage infiltration. Hyperplasia of type-2 pneumocytes was rarely seen, and bronchioloalveolar hyperplasia was not present in any of the NHP. There was minimal to mild interstitial fibrosis, typically associated with areas of inflammatory infiltration and proteinic fluid accumulation.

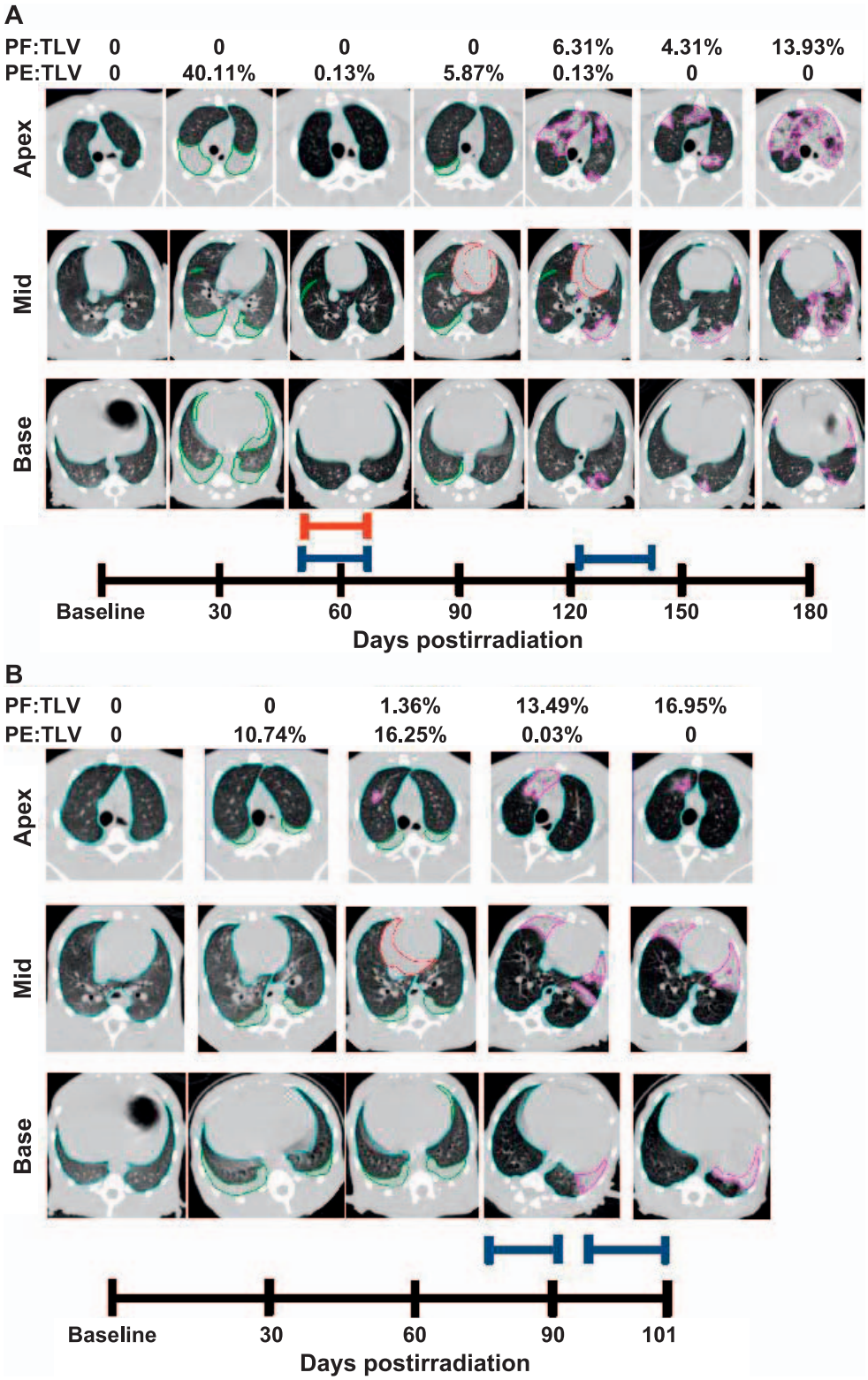

FIG. 5. Longitudinal CT analysis of a 10.74 Gy WTLI NHP, at baseline and followed every 30 days through the end of study. Transverse images taken at the apex, mid and base of lungs are shown in Fig. 4. Panel A: Total lung volume (TLV) is outlined in light blue, pleural effusion (PE) in green, pericardial effusion (PCE) in red and pneumonitis/fibrosis (PF) in pink. Quantitative results of PF:TLV and PE:TLV are given for each study day and represented as percentages of TLV. Pleural effusion and pneumonitis/fibrosis were observed at day 30–120 and day 120–180 postirradiation, respectively. Pericardial effusion was observed on day 90 and day 120, (21.68 ml and 9.77 ml, respectively). Furosemide (red bar) was administered on day 56–62 postirradiation for the presence of abdominal swelling per veterinary prescription. Dexamethasone (blue bars) was administered at day 54–62

TABLE 5
Radiographic Incidence of Pneumonitis/Fibrosis, Pulmonary Effusion and Pericardial Effusion in Rhesus Macaques after WTLI

Day after WTLI	Saline				AEOL 10150											
	Day 1–28				Day 1–28				Day 1–60				Day 1–28 plus day 60–80			
	n	PF (%)	PE (%)	PCE (%)	n	PF (%)	PE (%)	PCE (%)	n	PF (%)	PE (%)	PCE (%)	n	PF (%)	PE (%)	PCE (%)
30	20	20.0	60.0	0	20	55.0	50.0	0	20	30.0	75.0	0	20	60.0	60.0	0
60	16	43.8	50.0	37.5	16	75.0	56.3	12.5	18	66.7	55.6	33.3	18	77.8	44.4	41.7
90	13	76.9	23.1	15.4	15	86.7	40.0	6.7	16	87.5	62.5	12.5	12	91.7	41.7	8.3
120	11	100	54.5	9.1	10	70.0	20.0	10.0	16	100	31.3	0	10	100	60.0	20.0
150	8	100	50.0	0	7	71.4	57.1	0	12	100	41.7	0	8	100	50.0	0
180	8	80.0	40.0	0	7	57.1	28.6	0	10	80.0	20.0	0	5	100	60.0	0

Notes. Nonhuman primates received 10.74 Gy WTLI, and were then randomized among four cohorts [control (saline) and three AEOL 10150 treatment schedule cohorts] and observed for 180 days postirradiation. At least every 30 days postirradiation, CT scans were performed. The incidence of pneumonitis/fibrosis (PF), pulmonary effusion (PE) and pericardial effusion (PCE) observed on the CT scan in each treatment cohort is presented as a percentage of the number of animals alive at each time point postirradiation.

Day 67–99. The cellular infiltration noted in the earlier group was persistent. Hyperplasia of type-2 pneumocytes was noted with greater frequency, and there was a low incidence of bronchioloalveolar hyperplasia. Interstitial fibrosis was more common and pronounced relative to the earlier group.

Day 101–140. Histopathological alterations were generally similar to the earlier groups, though interstitial fibrosis was more common and pronounced.

Day 155–178. Histopathological alterations were generally similar to the earlier groups, but cellular infiltrations and accumulation of alveolar proteinic material were less common and less pronounced. However, the interstitial fibrosis and bronchioloalveolar hyperplasia were equivalent to the changes observed in the earlier groups.

Day 180–185. Histopathological alterations, including interstitial fibrosis, were generally similar to the preceding groups, though cellular infiltrations and accumulation of alveolar proteinic material were less common and less pronounced than seen in the earlier groups.

CONCLUSION

The H&E-stained sections from all treatment cohorts had a spectrum of changes that included accumulation of proteinic fluid in the alveoli, infiltrations of inflammatory cells (MNC, neutrophils, macrophages), type-2 pneumocyte and bronchioloalveolar hyperplasia. The trichrome-stained sections revealed interstitial fibrosis that was typically associated with infiltrations of inflammatory cells. The histological alterations were most pronounced in the upper and middle lobes of the lungs and tended to be of focal or multifocal distribution within each lung lobe.

Overview of Histological Changes

Histological changes were randomly scattered in the lungs, with no discernible pattern of distribution relative to lung surfaces, airways or vascular tracts. The lesions typically involved only portions of the lung lobes, with apparent sparing of other regions. There was substantial inter-animal variation in the histological character and severity of the lung lesions, but the following general pattern was apparent. The initial lung changes consisted of exudative pneumonitis, with accumulations of neutrophils and macrophages within alveolar lumina (Fig. 8A). Alveoli in affected areas were often lined with plump pneumocytes. Borders of affected areas were abrupt, with microscopically normal pulmonary tissue remaining in the immediately adjacent areas. The exudative lesions persisted for a considerable period, as shown in Fig. 8B (day 77) and Fig. 8C (day 122). The exudative lesions sometimes included intra-alveolar accumulations of homogeneous proteinic material, consistent with edema fluid or inflammatory transudate (Fig. 8B and C). Accumulation of collagen in alveolar walls, which was demonstrable with Masson's trichrome staining, was seen from the mid-to-late phases of the postirradiation period, and increased in prominence over time (Fig. 8C–F). Pronounced proliferation of epithelial cells, consistent with bronchioloalveolar hyperplasia, was also noted in the mid-to-late phases (Fig. 8D).

←
and day 121–146 postirradiation due to NSRR above 80 bpm in accordance with study protocol. Panel B: Longitudinal CT analysis of a NHP receiving 10.74 Gy WTLI at baseline and followed every 30 days through to early euthanasia on day 101 in accordance with study criteria. Total lung volume (TLV) is outlined in light blue, pleural effusion (PE) in green, pericardial effusion (PCE) in red and pneumonitis/fibrosis (PF) in pink. Quantitative results of PF:TLV and PE:TLV are given for each study day and represented as percentages of TLV. Pleural effusion and pneumonitis/fibrosis were observed at day 30–90 and at day 60–101 postirradiation, respectively. Pericardial effusion (13.08 ml) was observed on day 60. Dexamethasone (blue bars) administered at day 79–91 and day 93–101 postirradiation due to NSRR above 80 bpm according to study protocol.

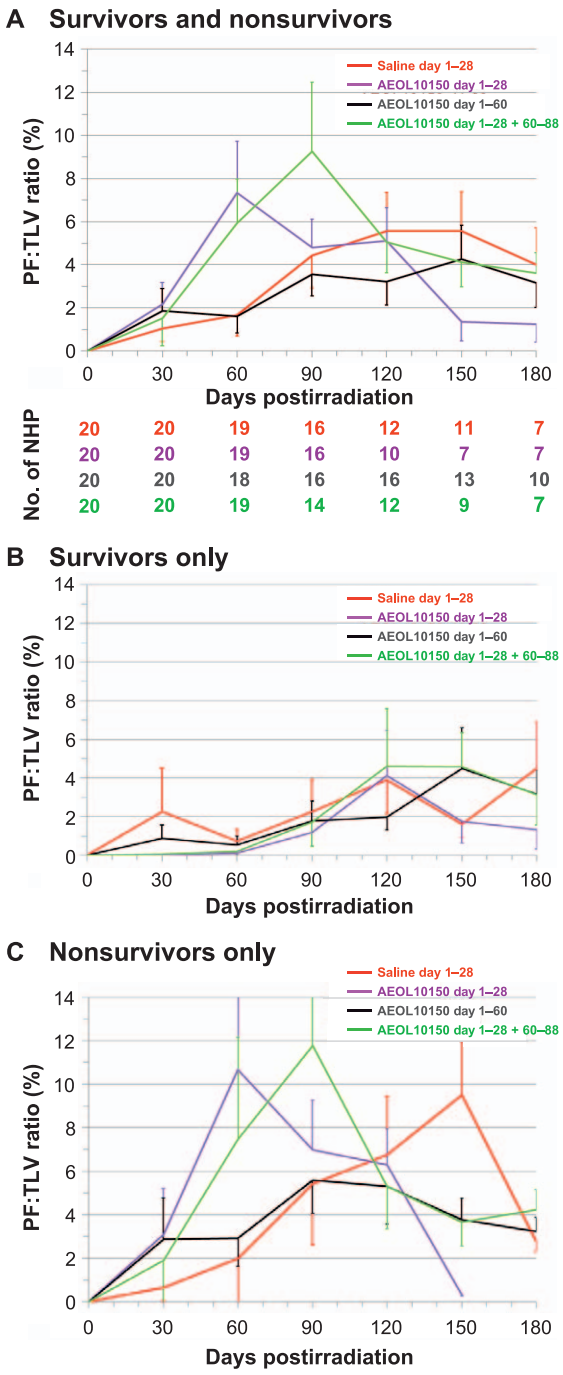

FIG. 6. Radiographic (CT) analysis of lung injury over time, showing the mean ratio of volume of pneumonitis/fibrosis indexed against the total lung volume (PF:TLV) as percentage and as a function of treatment after WTLI with the control (saline) and the AEOL 10150-treated cohorts (day 1–28, day 1–60 and day 1–28 plus day 60–88). CT scans were performed at baseline and every thirty days after WTLI until the end of study at 180 days or until the animal met euthanasia criteria. Scan results beyond day 30 on the graph are influenced by medical management with dexamethasone and ongoing morbidity and mortality of animals with the greatest pulmonary injury. Error bars represent SEM. Panels A–C: Comparisons of mean PF:TLV over time for all NHP survivors and nonsurvivors (panel A), survivors only (panel B) and nonsurvivors only (panel C) in the control cohort and each AEOL 10150-treated cohort. In panel A, the diminishing numbers of NHP are shown below each time point from baseline to day 180 postirradiation.

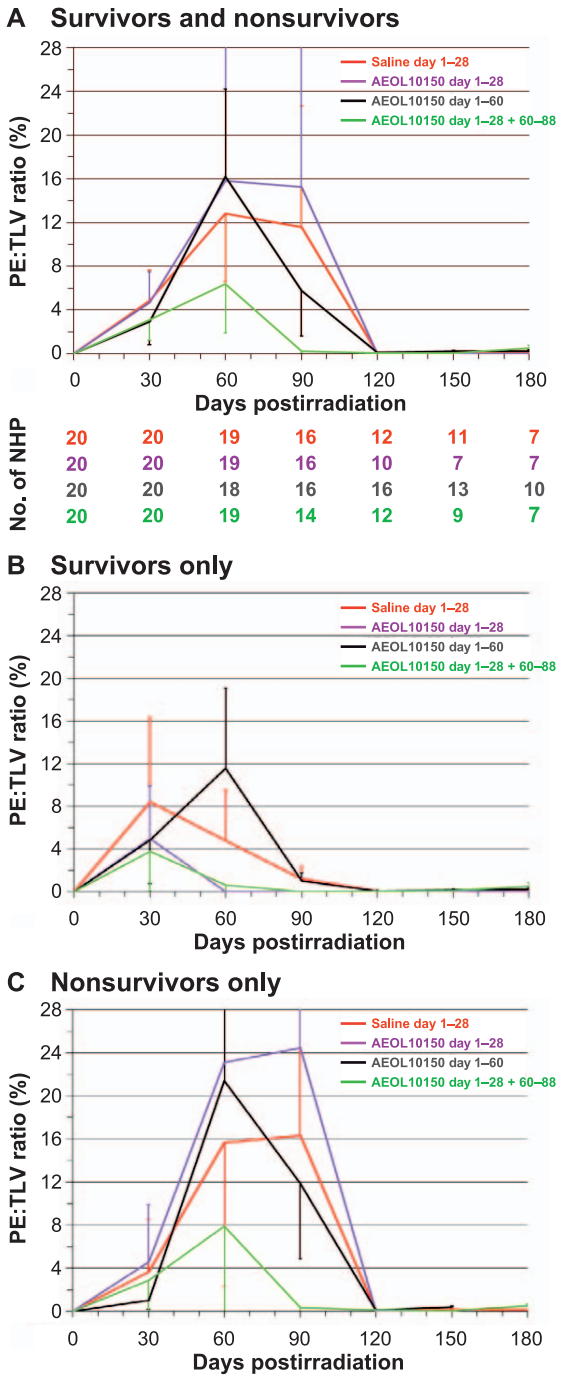

FIG. 7. Radiographic (CT) analysis of lung injury over time, showing the mean ratio of volume of pleural effusion indexed against the total lung volume (PE:TLV) as percentage and as a function of treatment after WTLI with the control (saline) and the AEOL 10150-treated cohorts (day 1–28, day 1–60 and day 1–28 plus day 60–88). CT scans were performed at baseline and every 30 days after WTLI until the end of study at 180 days or until the animal met euthanasia criteria. Scan results beyond day 30 on the graph are influenced by medical management with dexamethasone and ongoing morbidity and mortality of animals with the greatest pulmonary injury. Error bars represent SEM. Panels A–C: Comparison of mean PE:TLV over time for all NHP survivors and nonsurvivors (panel A), survivors only (panel B) and nonsurvivors only (panel C) in the control cohort and each AEOL 10150-treated cohort. Panel A shows diminishing numbers of NHP for each time point from baseline to day 180 postirradiation.

TABLE 6
Analysis of Wet Lung Weight to Body Weight (LW:BW) Ratio in 10.74 Gy WTLI Rhesus Macaques

Treatment	All	Survivors	Decedents
Saline (day 1–28)	1.533	1.397	1.578
AEOL 10150 (day 1–28)	1.497	1.344	1.568
AEOL 10150 (day 1–60)	1.322	1.306	1.341
AEOL 10150 (day 1–28 plus day 60–80)	1.566	1.388	1.613
Nonirradiated	1.000	1.000	1.000

Notes. After WTLI, animals were randomized among control (saline) and three AEOL 10150 treatment schedule cohorts and observed for 180 days postirradiation. Body weight and lung weight were collected at necropsy and the LW:BW ratio was calculated. The means of the LW:BW ratios were analyzed by treatment cohort as well as survivors and decedents per treatment cohort. The mean LW:BW ratio obtained from six naïve, nonirradiated rhesus macaques (0.815%) was defined as 1.00 and used as a nonirradiated comparator.

DISCUSSION

The Mortality versus Dose-Response Relationship for WTLI-Induced Lung Injury: A Model to Assess Injury and Treatment

The dose-response relationship for morbidity and mortality for the NHP exposed to whole-thorax lung radiation and administered medical management established a reliable model to assess MCM efficacy (*9, 10*). The prescribed midplane dose of WTLI, using 6 MV LINAC-derived photons, was a significant predictor of all-cause mortality in the 180-day study duration. All mortality in the WTLI model was secondary to RILI, highlighting the effectiveness of the model in isolating the pulmonary sub-syndrome from the acute hematopoietic and gastrointestinal subsyndromes, as well as multi-organ injury characteristic of the delayed effect of acute radiation exposure. The dose-response relationship over the dose range that characterized the dose-dependent morbidity and mortality associated with pulmonary injury provided the correct radiation dose of 10.74 Gy, associated with the $LD_{70/180}$ mortality required for the experimental design. A recent effort to establish specific organ-volume and dose received within a CT-defined anatomical structure will permit organ-specific dose-response relationships (*15, 16*). We also note that the dose-response relationship was established for the study duration of 180 days. We suggest an extension of the study duration in NHP to at least 270 days to establish a better estimate of progression and resolution of RILI.

The Primary End Point, Survival

The primary, clinically relevant parameter for a successful MCM is an increase in survival and/or mitigation of established key signs of morbidity assessed over the selected time course postirradiation (*8*). The current study demonstrated that AEOL 10150, administered on day 1–60 after WTLI, reduced several key signs of morbidity, increased survival and survival probability in a NHP model at 180 days after an expected, 70% lethal, RILI (Table 7). Administration of AEOL 10150, from day 1–60 after 10.74 Gy WTLI, an actual $LD_{75/180}$ herein, significantly improved cumulative survival by 25% over the 180-day study duration. The study protocol used here incorporated patient-based medical management that included administration of dexamethasone. The other two AEOL 10150 treatment schedules, day 1–28 and day 1–28 plus day 60–88, did not mitigate key signs of morbidity or mortality relative to the control cohort. These results suggested that the efficacy of AEOL 10150 required administration for a minimum of 60 consecutive days after WTLI. Analysis of the Kaplan-Meier plots and survival probability suggested that administration for an additional 30 days, from day 1–90, may be more effective in diminishing the extent of lung injury, reducing morbidity and further increasing survival and resolution of RILI.

AEOL 10150-Induced Efficacy, Secondary Parameters and Morbidity

Administration of AEOL 10150 in the day 1–60 schedule mitigated secondary parameters and key signs of morbidity, although not significantly so, along the entire time course of the RILI to the control cohort and other AEOL 10150 treatment schedules (Table 7). AEOL 10150 administered between day 1 to 60 after a 75% lethal WTLI dose increased mean and median survival time and time to onset of an NSRR $\geq$80 bpm, diminished wet lung weight of decedents at necropsy and increased SpO_2. However, it did not significantly diminish radiographic evidence of pneumonitis/fibrosis during the longitudinal study duration or clinical evidence assessed by NSRR and SpO_2. Additionally, the incidence and time course of pleural or pericardial effusion was not affected by the administration of AEOL 10150 in either schedule. Regardless of schedule, AEOL 10150 administration did not mitigate a number of secondary parameters, e.g., mean dexamethasone support, the early rise in radiographic evidence, incidence and extent of pneumonitis/fibrosis (PF:TLV) and pleural or pericardial effusions (PE:TLV, PCE:TLV).

The longitudinal analysis revealed the persistent progression of RILI in the control and all AEOL 10150 treatment cohorts after the 75% lethal dose of radiation that encompassed the lung and heart in WTLI (*15*). The 60-day administration schedule extended the short-term, 28-day schedules utilized previously to decrease mortality in rodent models and a NHP pilot study (*10, 34, 36*). Additionally, chronic administration of AEOL 10150 via osmotic mini-pumps showed increased efficacy relative to nonlethal end points when administered over 10 weeks relative to one week or control cohorts in a single, 28 Gy hemithorax model (*32*).

The data from this study suggest that increased efficacy against RILI and mortality consequent to 10.74 Gy WTLI will require more prolonged administration of AEOL 10150

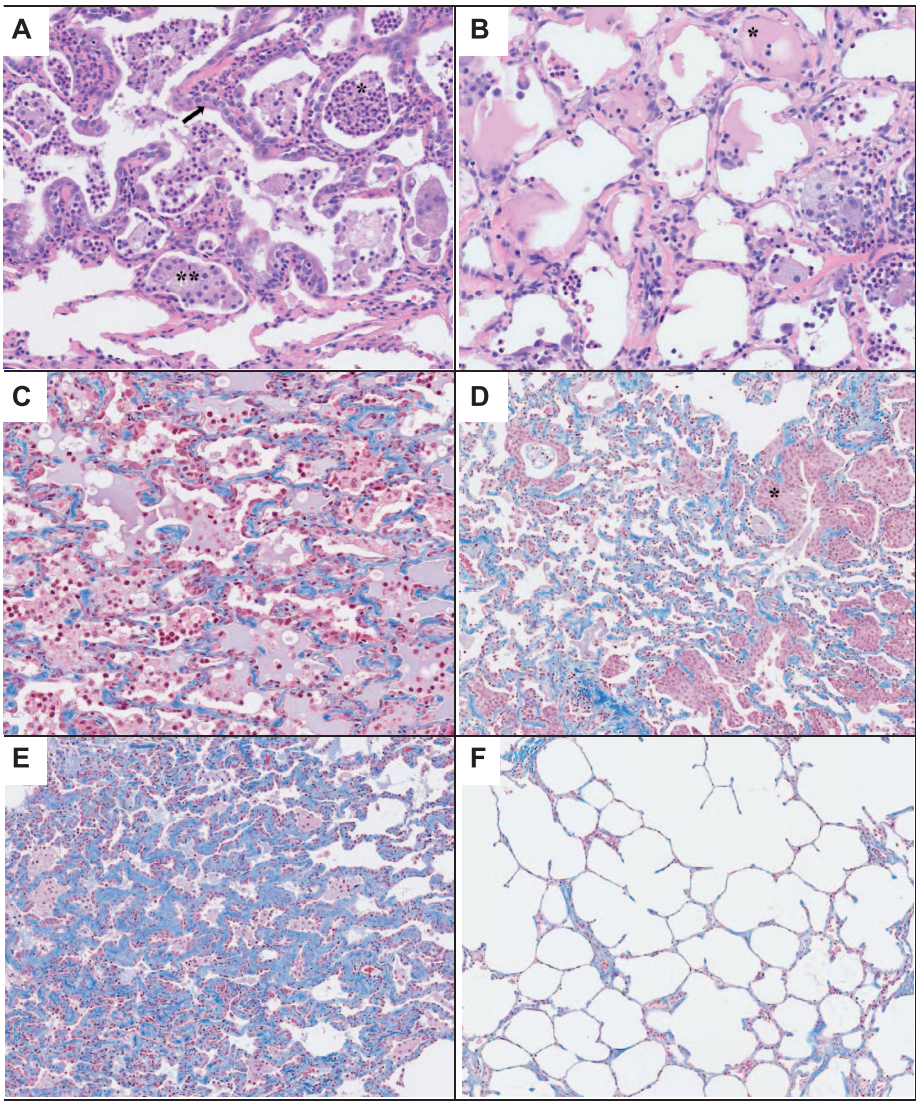

FIG. 8. Panels A–F: Representative fields of lung tissue histology from control and AEOL 10150-treated NHP after 10.74 Gy WTLI. Radiation-induced histological damage was not distinguishable among control and AEOL 10150-treated cohorts. Panel A: Lung of a rhesus macaque collected at day 56 postirradiation. A well-defined area has thickened alveolar walls and alveolar lumina filled with neutrophils (*) and macrophages (**). Alveoli are lined by a single layer of plump pneumocytes (arrow). Note the abrupt border between the lesion area and the thin alveolar walls of the normal lung tissue at the bottom of the image. H&E stain, 20× objective magnification. Panel B: Lung of a rhesus macaque collected at day 77 postirradiation. Alveoli contain a mixed population of inflammatory cells, with neutrophils and macrophages predominating. Some alveoli (*) contain a moderate amount of homogeneous eosinophilic material that is consistent with edema fluid protein or an inflammatory transudate. H&E stain, 20× objective magnification. Panel C: Lung of a rhesus macaque collected at day 122 postirradiation. Alveoli contain a mixed population of inflammatory cells intermixed with homogeneous proteinic material. Alveolar walls are slightly thickened by the presence of blue-stained collagen. Masson's trichrome stain, 20× objective magnification. Panel D: Lung of a rhesus macaque collected at day 129 postirradiation. Inflammatory cell infiltration is not pronounced, but alveolar walls contain a moderate amount of blue-stained collagen. Note the extensive areas of epithelial cell proliferation (*). Masson's trichrome stain, 10× objective magnification. Panel E: Lung of a rhesus macaque collected at day 178 postirradiation. Inflammatory cell infiltration is minimal, but alveolar walls are markedly thickened by the presence of blue-stained collagen. Note that many alveoli are lined by plump cuboidal pneumocytes, compared to the thin squamoid pneumocytes that typically line alveoli. Masson's trichrome stain, 10× objective magnification. Panel F: Lung of rhesus macaque collected at day 178 postirradiation. This is from the same animal as shown in panel E, but the section is from a different lung lobe. Note the thin alveolar walls lined by thin, virtually invisible pneumocytes and the minor amount of blue-stained collagen in alveolar walls. Masson's trichrome stain, 10× objective magnification.

TABLE 7
Compilation of Parameters Improved by AEOL 10150 Treatment when Administered on Day 1–60, after WTLI in NHP

Parameter	Improvement
Survival	Increased vs. saline (control) and AEOL 10150 cohorts, day 1–28 or day 1–28 plus day 60–88
Kaplan-Meier	Increased survival over 180 days
Overall survival time	Increased mean and median
Survival time of decedents	Increased mean and median
NSRR $\geq$60, $\geq$80	Increased the latency, mean and median
NSRR $\geq$60, $\geq$80	Increased time to day 1, mean and median
Dexamethasone support	Increased time to onset/treatment, mean and median
SpO_2	Trend toward higher values
PF:TLV	Less quantitative lung injury over time after WTLI
Lung wet weight	Mean value less relative to all animals as well as within survivors and decedents

Notes. Rhesus macaques received 10.74 Gy WTLI using 6 MV LINAC-derived photons at a dose rate of 0.80 Gy/min. Animals were administered AEOL 10150 in three different treatment schedules and observed for 180 days postirradiation. Survival, nonsedated respiration rates (NSRR), corticosteroid requirements, oxygen saturation (SpO_2), radiographic analysis [incidence of pneumonitis/fibrosis (PF) to total lung volume (TLV] and the wet lung weight are shown.

through at least 90 days postirradiation. The overall incidence, severity and progression of morbidity and mortality appeared intractable when revealed by the longitudinal analysis. The Kaplan-Meier survival function provided an analysis of the earliest mortality that could be linked to that of key clinical signs and radiographic evidence of lung injury. The 60-day schedule mitigated the early mortality noted over the subsequent 30 days, from 60–90 days and significantly diminished the progression of mortality through 90 days postirradiation, e.g., the slope relative to loss of survival probability relative to the control cohort and that of the other AEOL 10150-treated cohorts was significantly diminished through survival outcome at 180 days. It is of interest that the slope for progression of mortality from 90–180 days was not significantly different from that of the control cohort. The progression of mortality for the day 1–60 AEOL 10150-treated cohort remained equivalent to that of the control cohort through the remaining 90 days to the end of the study. The mechanism for RILI at the $LD_{70/180}$ dose is persistent. These data suggest that continued administration for an additional 30 days would further mitigate the incidence and extent of lung injury and thus mitigate mortality to a more significant outcome over the 180-day study duration.

A NHP Model of WTLI-Induced Lung Injury and Treatment

The NHP model of WTLI correlates well with what is known about the human response to acute, high-dose radiation exposure. Reports of humans receiving a single, high-dose whole-thorax exposure in a controlled clinical situation are rare. The most relevant experience has been reported by the Princess Margaret Hospital (*41, 42*). The clinical database included a total of 245 metastatic cancer patients who received single upper half-body irradiation (UHBI) (prescribed to midplane), ranging between 2.0 and 10.0 Gy, for palliation of thoracic metastases. Forty-four of the 245 patients eventually developed acute radiation pneumonitis. The median time to pneumonitis was 100 days postirradiation (*41*). Radiation-induced pneumonitis was observed in over 90% of the patients exposed to either 8 or 10 Gy. The incidence of pneumonitis observed in UHBI patients that received 8 or 10 Gy was not reduced with increasing radiation dose. The reasons for this finding may be that over 90% of the cases were seen in one of only two dose levels, along with the potentially confounding nature of the study population (terminal cancer patients with thoracic malignancies, concomitant chemotherapy and other therapies). For NHP, the average latency to onset of clinical pneumonitis after WTLI was inversely related to radiation dose, and ranged from 63.0 days (12.0 Gy) to 119.6 days (9.5 Gy), with a stepwise gradient across the dose range (*9*). The average time to clinical manifestation of lung injury in the model development for WTLI-induced lung injury for doses of 10.5 and 11.0 Gy, which bracketed the 10.74 Gy dose used herein, was approximately 90–95 days postirradiation (*9*). In the previously reported AEOL 10150 pilot study using 11.5 Gy WTLI, the mean time to an NSRR $\geq$80 bpm to trigger dexamethasone treatment was 76 days (*10*). In the current study, the mean time to NSRR $\geq$80 bpm for the control cohort was 78 days. The incidence of radiation pneumonitis increased with radiation dose in both humans and NHP, and the dose-response relationship is comparably steep between species (*9, 41–43*). The incidence of pneumonitis in the NHP WTLI model (62.5% at 10.0 Gy) is similar to that observed in the human experience (52% at 10.0 Gy). Based on the probit analysis of absolute lung dose versus incidence of radiation pneumonitis, Van Dyk *et al.* reported that the onset of radiation pneumonitis occurred at approximately 8.0 Gy and increased rapidly until reaching 100% at approximately 11.0 Gy (*41*). Others have reported a more restricted analysis of patients from the same clinical trial series with good clinical symptomology and radio-

graphic follow-up, and suggested the threshold in humans is >8 Gy (*43*). The lethality in patients who developed pneumonitis was 84% (37/44) despite treatment. For NHP, the onset of radiation pneumonitis was seen at 9.5 Gy and increased rapidly until reaching 100% at a lethal dose of 11.5 Gy (*9*). The incidence of pneumonitis observed in NHP exposed to 10.5 or 11.0 Gy was 70 or 90%, respectively. Herein, exposure to 10.74 Gy induced evidence of pneumonitis/fibrosis radiographically in 100% of the control cohort. Of the NHP that developed pneumonitis in the dose-response relationship study, 70% (21/30) of the cases were lethal relative to 75% mortality in the control cohort noted herein (*9*). It should be noted that the NHP model was comprised of young healthy subjects versus terminal cancer patients, therefore such comparisons are difficult and must be made in the context of acknowledging the potential confounding variables (radiation quality, dose rate, concomitant medications, concomitant thoracic disease and performance status).

The collection of published data from radiation accidents has provided further evidence of the 9–10 Gy dose range for RILI and the ability of patients to survive high-dose exposure and ARS due to the nonuniform and/or heterogeneous nature of the exposures and adequate medical management (*1, 2, 44*). Hematopoietic growth factors (cytokines) were used to treat early H-ARS in each of these accidents. The role of early growth factor administration on evolution of early organ-specific sequelae and the latency, incidence, severity, progression and resolution of multi-organ injury is unknown and is a key question in the continuing development and approval of MCM to treat personnel in the radiation terrorist scenario (*45*).

A NHP Model with Medical Management, Dexamethasone

Dexamethasone treatment as a component of medical management may have a significant influence on the time course of morbidity and mortality. Published studies of rodent models have suggested that steroids have a protective or mitigating effect against radiation pneumonitis and may influence survival after whole-thorax irradiation to the lungs and heart (*37–40, 46*). Gross *et al*., reported that after acute lethal whole-thorax irradiation, administration of methylprednisolone on alternate days from 80–100 days postirradiaiton and then daily thereafter had an impact on survival during the time steroids were being administered (*37*). Animals receiving corticosteroids had an increased survival time relative to the nontreated cohort. Additionally, corticosteroid administration significantly enhanced survival at 19 weeks postirradiation. However, overall survival through 21 weeks was equivalent when the steroids were discontinued at 19 weeks. Gross *et al*. also found that administration of methylprednisolone initiated at week 11 postirradiation increased the LD_{50} (assessed at 26 weeks) from 14.3 to 17.6 Gy, resulting in a protection factor of 1.2 (*37*). Geraci *et al*. demonstrated that administration of dexamethasone reduced radiation-induced injury in an organ- or tissue-specific manner in a rat model of partial-body irradiation (22.5 Gy) (*40*). Dexamethasone provided through drinking water after partial-body irradiation increased the median survival time (63 days to 150 days) and eliminated lethal accumulation of pleural fluid. These studies suggested that steroid treatment may mitigate radiation-induced morbidity, survival time and mortality. The established NHP model of WTLI-induced lung injury used a treatment protocol that included individual administration of dexamethasone based on clinical signs (*9*). The effect of steroid-deficient medical management on morbidity and mortality over 180 days has not been determined. In contrast to the rodent studies that do not use steroid-based supportive care, the patient-based steroid treatment was administered as a planned taper over several weeks, similar to the clinical treatment paradigms after thoracic radiation-induced pneumonitis (*46*). The clinical treatment paradigm in the context of the high-dose nuclear radiation scenario will very likely include administration of steroids as a part of the standard of care and administration of MCM, given the evidence of radiation pneumonitis.

Heart and Lung Interaction: A Strategic Approach to Radiation-Induced Combined Organ Injury

The concomitant exposure of the heart is an additional risk factor with the lung damage induced by thoracic irradiation (*11–14, 17*). In their published study using high-precision proton beams, Van Luijk *et al*. suggested that when the heart was exposed to 20 Gy, tolerance to radiation-induced injury was reduced in the lung. Furthermore, the irradiated heart had an early damage component that may occur concomitantly with the latent phase of lung injury (*13*). These results provided a cautionary note that a ''...more severe acute and delayed toxicity should be expected after combined lung and heart irradiation'' (*11*). The WTLI model employs a near-uniform and homogeneous radiation exposure in an effort to marginalize dose–volume effects in both lung and heart (*11, 14, 15*). Medhora *et al*. reported on additional evidence of the complex interaction of radiation-induced effects on function and structure of the lung and heart in a rat model consequent to WTLI. They further suggested a potential role for angiotensin-converting enzyme inhibitors to mitigate combined lung and heart injury (*17*). In their published study, van der Veen *et al*. suggested that captopril diminished the ''...heart component of thoracic irradiation-induced damage...'' and therefore diminished ''...its effect on total early cardiopulmonary damage...'' (*47*). They further suggested that retrospective studies of clinical exposure protocols for patients that received angiotensin-converting enzyme inhibitors be conducted to assess the dose to the heart and potential mitigation of heart injury and effect on RILI. In this regard, Prado *et al*. used a retrospective, CT-based, heterogeneity-corrected dose calculation to estimate mean

dose to the lung and heart within the contoured organ volume corresponding to the prescribed mid-thorax dose in the NHP used in the current study (*15*). It was shown that dose gradients did exist within each organ and that the mean dose to the lung and heart were 11.05 Gy and 10.77 Gy, respectively, relative to the prescribed mid-thorax dose of 10.74 Gy. Animal models of lung injury, WTLI or partial-body exposure with bone marrow sparing, will provide an unparalleled opportunity to assess the interaction of heart and lung in combined or multi-organ injury relative to a more strategic approach to assessing the delayed effects of high-dose, acute radiation exposure and MCM efficacy.

ACKNOWLEDGMENTS

Funding for this study was provided by Aeolus Pharmaceuticals, Inc. under Biomedical Advanced Research and Development Authority (BARDA) contract no. HHSO100201100007C and in part from the National Institute of Allergy and Infectious Diseases (NIAID), through the MCART, Radiation/Nuclear Medical Countermeasure Product Development Support Services under contract no. HHSN272201000046C.

Received: February 10, 2016; accepted: November 28, 2016; published online: February 16, 2017

REFERENCES

1. Baranov AE, Selidovkin GD, Butturini A, Gale RP. Hematopoietic recovery after 10-Gy acute total body radiation. Blood 1994; 83:596–9.
2. Uozaki H, Fukayama M, Nakagawa K, Ishikawa T, Misawa S, Doi M et al. The pathology of multi-organ involvement: two autopsy cases from the Tokai-mura criticality accident. Br J Radiol 2005; 27:13–16.
3. Asano S. Multi-organ involvement: lessons from the experience of one victim of the Tokai-mura criticality accident. Br J Radiol 2005; 78.
4. Dainiak N, Gent RN, Carr Z, Schneider R, Bader J, Buglova E, et al. Literature review and global consensus on management of acute radiation syndrome affecting nonhematopoietic organ systems. Disaster Med Public Health Prep 2011; 5:183–201.
5. Guskova AK, Nadezhina N, Barabanova AV, Baranov AE, Gusev IA, Protasova TG, et al. Acute effects of radiation exposure following the Chernobyl acident, Immediate results of radiation sickness and outcome of treatment. In: Browne D, Weiss JF, MacVittie TJ, Pillai MV, editors. Treatment of radiation injuries. New York: Plenum Press; 1990. p. 195–209.
6. Dainiak N, Gent RN, Carr Z, Schneider R, Bader J, Buglova E, et al. First global consensus for evidence-based management of the hematopoietic syndrome resulting from exposure to ionizing radiation. Disaster Med Public Health Prep 2011; 5:202–12.
7. Crawford LM, Food and Drug Administration. New drug and biological drug products; evidence needed to demonstrate effectiveness of new drugs when human efficacy studies are not ethical or feasible. 21 CFR Pt. 314 and 601. Federal Register 2002; 67: 37988–98. (http://bit.ly/1Bq3SJJ)
8. Product development under the animal rule: guidance for industry. Center for Drug Evaluation and Research, Food and Drug Administration; Silver Spring, MD, 2015. (http://bit.ly/2knVRsn)
9. Garofalo M, Bennett A, Farese AM, Ward A, Taylor-Howell C, Cui W, et al. The delayed pulmonary syndrome following acute high-dose irradiation: a rhesus macaque model. Health Phys 2014; 106:56–72.
10. Garofalo MC, Ward AA, Farese AM, Bennett A, Taylor-Howell C, Cui W, et al. A pilot study in rhesus macaques to assess the treatment efficacy of a small molecular weight catalytic metallo-porphyrin antioxidant (AEOL 10150) in mitigating radiation-induced lung damage. Health Phys 2014; 106:73–83.
11. Novakova-Jiresova A, van Luijk P, van Goor H, Kampinga HH, Coppes RP. Pulmonary radiation injury: identification of risk factors associated with regional hypersensitivity. Cancer Res 2005; 65:3568–76.
12. Ghobadi G, van der Veen S, Bartelds B, de Boer RA, Dickinson MG, de Jong JR, et al. Physiological interaction of heart and lung in thoracic irradiation. Int J Radiat Oncol Biol Phys 2012; 84:e639–46.
13. van Luijk P, Novakova-Jiresova A, Faber H, Schippers JM, Kampinga HH, Meertens H, et al. Radiation damage to the heart enhances early radiation-induced lung function loss. Cancer Res 2005; 65:6509–11.
14. van Luijk P, Faber H, Meertens H, Schipper JM, Langendijk JA, Brandenburg S, et al. The impact of heart irradiation on dose-volume effects in the rat lung. Int J Radiat Oncol Biol Phys 2007; 69: 552–9.
15. Prado C, Kazi A, Bennet AW, MacVittie TJ, Prado K. Mean organ doses resulting from non-human primate whole thorax lung irradiation prescribed to mid-line tissue. Health Phys 2015; 109: 367–73.
16. de Faria EB, Barrow K, Ruehle BT, Parker JT, Swartz E, Taylor-Howell C, et al. The evolving MCART multimodal imaging core: Establishing a protocol for computed tomography and echocardiography in the rhesus macaque to perform longitudinal analysis of radiation-induced organ injury. Health Phys 2015; 109:479–92.
17. Medhora M, Gao F, Glisch C, Narayanan J, Sharma A, Harmann LM, et al. Whole-thorax irradiation induces hypoxic respiratory failure, pleural effusions and cardiac remodeling. J Radiat Res 2015; 56:248–60.
18. Vujaskovic Z, Batinic-Haberle I, Rabbani ZN, Feng QF, Kang SK, Spasojevic I, et al. A small molecular weight catalytic metalloporphryin antioxidant with superoxide dosmutase (SOD) mimetic properties protects lungs from radiation-induced injury. Free Radic Biol Med 2002; 33:857–63.
19. Rabbani ZN, Salahuddin FK, Yarmolenko P, Batinic-Haberle I, Thrasher BA, Gauter-Fleckenstein B, et al. Low molecular weight catalytic metalloporphyrin antioxidant AEOL 10150 protects lungs from fractionated radiation. Free Radic Res 2007; 41:1273–82.
20. Flechsig P, Dadrich M, Bickelhaupt S, Jenne J, Hauser K, Timke C, et al. LY2109761 attenuates radiation-induced pulmonary murine fibrosis via reversal of TGFb and BMP-associated proinflammatory and proangiogenic signals. Clin Cancer Res 2012; 18:3616–27.
21. Wang Q, Usinger W, Nichols B, Gray J, Xu L, Seeley TW, et al. Cooperative interaction of CTGF and TGF-b in animal models of fibrotic disease. Fibrogenesis Tissue Repair 2011; 4:4.
22. Huber PE, Bickelhaupt S, Peschke P, Tietz A, Wirkner U, Lipson KE. Reversal of established fibrosis by treatment with the anti-CTGF monoclonal antibody FG-3019 in a murine model of radiation-induced pulmonary fibrosis. Am J Respir Crit Care Med 2010; 181:A1054.
23. Lipson KE, Wong C, Teng Y, Spong S. CTGF is a central mediator of tissue remodeling and fibrosis and its inhibition can reverse the process of fibrosis. Fibrogenesis Tissue Repair 2012; 5:S24.
24. Alapati D, Rong M, Chen S, Hehre D, Rodriguez MM, Lipson KE, et al. Connective tissue growth factor antibody therapy attenuates hyperoxia-induced lung injury in neonatal rats. Am J Respir Cell Mol Biol 2011; 45:1169–77.
25. Gao F, Fish BL, Szabo A, Doctorow SR, Kma L, Molthen RC, et al. Short-term treatment with a SOD/catalase mimetic, EUK-207, mitigates pneumonitis and fibrosis after single-dose total-body or whole thoracic irradiation. Radiat Res 2012; 178:468–80.
26. Epperly M, Bray J, Kraeger S, Zwacka R, Greenberger J. Prevention of late effects of irradaiation lung damage by manganese superoxide dismutase gene therapy. Gene Therapy 1998; 5:196–208.

27. Abdollahi A, Li M, Ping G, Plathow C, Domhan S, Kiessling F, et al. Inhibition of platelet-derived growth factor signaling attenuates pulmonary fibrosis. J Exp Med 2005; 201:925–35.
28. Srour N, Thebaud B. Mesenchymal stromal cells in animal bleomycin pulmonary fibrosis models: A systematic review. Stem Cells Transl Med 2015; 4:1500–10.
29. Fang X, Abbott J, Cheng L, Colby JK, Lee JW, Levy BD, et al. Human mesenchymal stem (stromal) cells promote the resolution of acute lung injury in part through lipoxin A4. J Immunol 2015; 195:875–81.
30. Riley PA. Free radicals in biology: Oxidative stress and the effects of ionizing radiation. Int J Radiat Oncol Biol Phys 1994; 65:27–33.
31. Schaue D, Kachikwu EL, McBride WH. Cytokines in radiobiological responses: a review. Radiat Res 2012; 178:505–23.
32. Rabbani ZN, Batinic-Haberle I, Anscher MS, Huang J, Day BJ, Alexander E, et al. Long-term administration of a small molecular weight catalytic metalloporphyrin antioxidant, AEOL 10150, protects lungs from radiation-induced injury. Int J Radiat Oncol Biol Phys 2007; 67:573–80.
33. Gauter-Fleckenstein BG, Fleckenstein K, Owzar K, Jiang C, Reboucas JS, Batiric-Haberle I, et al. Early and late administration of MnTE-2-PyP5+ in mitigation and treatment of radiation-induced lung damage. Free Radic Biol Med 2010; 48:1034–43.
34. Murigi FN, Mohindra P, Hung C, Salimi S, Goetz W, Pavlovic R, et al. Dose optimization study of AEOL 10150 as a mitigator of radiation-induced lung injury in CBA/J mice. Radiat Res 2015; 184:422–32.
35. MacVittie TJ, Bennett A, Booth C, Garofalo M, Tudor G, Ward A, et al. The prolonged gastrointestinal syndrome in rhesus macaques: the relationship between gastrointestinal, hematopoietic, and delayed multi-organ sequelae following acute, potentially lethal, partial-body irradiation. Health Phys 2012; 103:427–53.
36. Jackson IL, Zhang X, Hadley C, Rabbani ZN, Zhang Y, Marks S, et al. Temporal expression of hypoxia-regulated genes is associated with early changes in redox status in irradiated lung. Free Radic Biol Med 2012; 53:337–46.
37. Gross NJ. Radiation pneumonitis in mice. Some effects of corticosteroids on mortality and pulmonary physiology. J Clin Invest 1980; 66:504–10.
38. Gross NJ, Narine KR, Wade R. Protective effect of corticosteroids on radiation pneumonitis in mice. Radiat Res 1988; 113:112–9.
39. Phillips TL, Wharam MD, Margolis LW. Modification of radiation injury to normal tissues by chemotherapeutic agents. Cancer 1975; 35:1678–84.
40. Geraci JP, Mariano MS, Jackson KL, Taylor DA, Still ER. Effects of dexamethasone on late radiation injury following partial-body and local organ exposures. Radiat Res 1992; 129:61–70.
41. Van Dyk J, Keane TJ, Kan S, Rider WD, Fryer CJ. Radiation pneumonitis following large single dose irradiation: a re-evaluation based on absolute dose to lung. Int J Radiat Oncol Biol Phys 1981; 7:461–7.
42. Fryer CJH, Fitzpatrick PJ, Rider WD, Poon P. Radiation pneumonitis: experience following a large single dose of radiation. Int J Radiat Oncol 1978; 4:931–6.
43. Prato FS, Kurdyak R, Saibil EA, Carruthers JS, Rider WD, Aspin N. The incidence of radiation pneumonitis as a result of single fraction upper half body irradiation. Cancer 1977; 39:71–8.
44. The radiological accident in Samut Prakarn. IAEA, 2002. Vienna: International Atomic Energy Agency; 2002. (http://bit.ly/2jmIzKV)
45. MacVittie TJ, Bennett AW, Farese AM, Taylor-Howell C, Smith CP, Gibbs AM, et al. The effect of radiation dose and variation in Neupogen(R) initiation schedule on the mitigation of myelosuppression during the concomitant GI-ARS and H-ARS in a nonhuman primate model of high-dose exposure with marrow sparing. Health Phys 2015; 109:427–39.
46. Berkely FJ. Managing the adverse effects of radiation therapy. Am Fam Physician 2010; 82:381–8.
47. van der Veen SJ, Ghobadi G, de Boer RA, Faber H, Cannon MV, Nagle PW, et al. ACE inhibition attenuates radiation-induced cardiopulmonary damage. Radiother Oncol 2015; 114:96–103.